



# Tuning the properties of ionic liquids by mixing with organic solvents: The case of 1-butyl-3-methylimidazolium glutamate with alkanols



H. Ghazipour<sup>a</sup>, A. Gutiérrez<sup>b</sup>, M.M. Alavianmehr<sup>a</sup>, S.M. Hosseini<sup>c,\*</sup>, S. Aparicio<sup>b,\*</sup>

<sup>a</sup> Department of Chemistry, Shiraz University of Technology, Shiraz 71555-313, Iran

<sup>b</sup> Department of Chemistry, University of Burgos, 09001 Burgos, Spain

<sup>c</sup> Department of Chemistry, University of Hormozgan, Bandar Abbas 71961, Iran

## ARTICLE INFO

### Article history:

Received 31 May 2021

Revised 30 September 2021

Accepted 24 October 2021

Available online 25 November 2021

### Keywords:

Aminoacid ionic liquid

Alkanols

Liquid mixtures

Hydrogen bonding

Quantum chemistry

Molecular dynamics

## ABSTRACT

Binary liquid mixtures of 1-butyl-3-methylimidazolium glutamate acid ([bmim][glu]) with alkanols (1-propanol, isobutanol and 1,2-propanediol) are studied in the full composition range as a function of temperature using a combined experimental and computational chemistry approach. Experimental thermo-physical information as well as derived excess and mixing properties allowed to characterize these complex liquid mixtures in terms of deviation from ideality as well their relationships with the developed intermolecular forces and changes with the type of considered alkanols. Theoretical studies using quantum chemistry and classical molecular dynamics simulations provided nanoscopic characterization on the studied fluids, with particular attention to the extension and nature of hydrogen bonding and its effects on molecular arrangements and mixed fluids' properties. The reported study provides a micro and macroscopic characterization of the considered aminoacid-based ionic liquid mixtures, thus contributing to the knowledge of sustainable ionic liquid systems mixed with organic solvents for fine tuning properties and developing task specific applications.

© 2021 The Authors. Published by Elsevier B.V. This is an open access article under the CC BY-NC-ND license (<http://creativecommons.org/licenses/by-nc-nd/4.0/>).

## 1. Introduction

The academic and industrial interests in Ionic liquids (ILs) are growing rapidly over the last years because of their possible applications in a large collection of technologies [1,2]. However, those possibilities have suffered some drawbacks [3-5] because of reported problems in terms of toxicity [6], biodegradability and environmental fate [7,8]. These problems and the search for truly green and sustainable solvents [9] have at least partially shifted the interest in ILs to closely related fluids such as Deep Eutectic Solvents (DES) [10], which are proposed to be more suitable and sustainable fluids [11,12] being used for a large collection of technological applications [13]. Nevertheless, the large number of anion – cation combinations leading to the formation of ILs also allows to search and develop ILs with better properties [14-16]. Among this group, aminoacid – based ILs (AAILs) [17] have attracted attention because of their suitable properties, such as thermal stability [18], moderate viscosity [19-21] and suitable biodegradability paired with low toxicity [22,23], although certain toxicity has been reported for some types of AAILs [24]. Likewise,

AAILs have been successfully considered for a wide range of technological applications such as CO<sub>2</sub> capture [25], lubrication [26], biomolecular stabilization [27] or drug delivery [28] among others.

The IL platform to develop suitable technological applications can be further extended by the consideration of ILs mixtures, both IL – IL mixtures [29,30] as well as IL – molecular solvents (MSs) mixtures [31-33], including water-containing mixtures [34-36]. The interest in ILs + MSs mixtures [37-39] stands on the possibility of fine tuning ILs properties through the combination with suitable amounts of MSs, i.e. physicochemical properties design through mixture composition [37,40-42]. In this way, some of the most relevant problems on the scalability of ILs to industrial level [43], such as their high viscosity [44], maybe overcome [45]. Nevertheless, the available knowledge on IL + MS mixtures, both from the micro and macroscopic viewpoints, is still scarce. The large number of factors to be considered for the development of IL + MS mixtures, i.e. type of ions, type of MS, mixtures composition, pressure and temperature, to mention ones, makes it necessary to understand the fluids' behaviour and properties as well as for the development of structure – property relationships as well as predictive methods, which can be used for practical applications of IL + MS mixtures [46-48]. In spite of the relevance of IL + MS mixtures, most of the available studies are concentrated in alkylimidazolium –

\* Corresponding authors.

E-mail addresses: [sm.hosseini@hormozgan.ac.ir](mailto:sm.hosseini@hormozgan.ac.ir) (S.M. Hosseini), [sapar@ubu.es](mailto:sapar@ubu.es) (S. Aparicio).

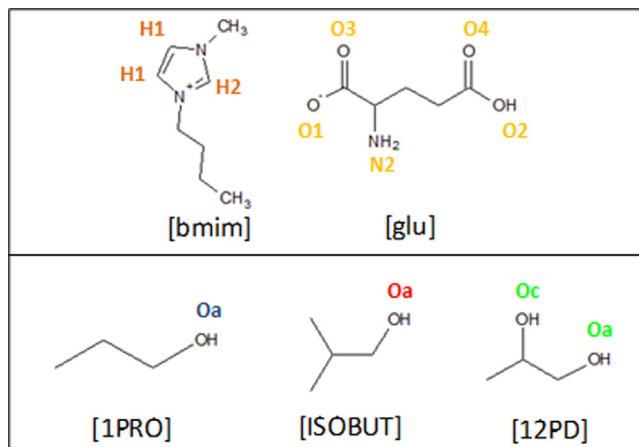


**Fig. 1.** Molecular structures of compounds used in this work. Red labels indicate atomic sites naming using along this work. (For interpretation of the references to color in this figure legend, the reader is referred to the web version of this article.)

based ILs with MSs such as water [49], alkanols [50], acetonitrile [51] and others [52]. The studies on other types of ILs such as ammonium- [53] or phosphonium- [54] based ones for MS mixtures are present in the literature but the consideration of other types of ions for ILs + MS mixtures should be studied, for the sake of more suitable physicochemical properties as well as sustainability considerations. Nevertheless, AAILs have been shortly considered for ILs + MS mixtures [55] in spite of the aforementioned suitable properties of this type of IL. AAILs mixtures with water have been recently considered for environmental applications such as pesticides degradation [56] whereas mixtures with organic solvents such as alkanol [57] have been considered. Therefore, with the objective in advancing in the knowledge of AAILs + MS mixtures, the 1-butyl-3-methylimidazolium glutamate IL ([bmim][glu]) was considered and their mixtures with selected alkanols (1-propanol, 1PRO; isobutanol, ISOBUT; 1,2-propanediol, 12PD) were studied in this work, Fig. 1. The considered [glu] anion is included in the list of non-toxic pharmaceutically acceptable anions [58], thus providing a suitable non-toxic alternative to other ions, thus fulfilling the recommendations for developing greener ILs [8]. Likewise, it is well-known that AAILs maybe produced at a lower cost than other conventional ILs [59], which is a key factor for the scalability of ILs-based technologies. The available literature shows studies on [bmim][glu] properties, such as density (showing a dense fluid with 1.2292 g cm<sup>-3</sup> at 298.15 K [60]), surface tension (60.8 mJ m<sup>-2</sup> at 298.15 [58]) as well as property estimation

methods [61]. Nevertheless, studies [bmim][glu] + MS mixtures are absent in the literature. Therefore, a combined (thermophysical) experimental and molecular modelling study (quantum chemistry and classical molecular dynamics simulations) is reported in this work to characterize [bmim][glu] + {1PRO or ISOBUT or 12PD} as a function of mixture composition and temperature. The study provides a micro and macroscopic characterization of the studied systems, the developed intermolecular forces and the factors controlling the properties of the considered complex mixtures. The properties of the studied mixtures in terms of deviations from ideality will be studied using excess properties. The pivotal role of intermolecular hydrogen bonding on the mixed fluids' structuring will be also characterized. Therefore, this contribution would extend the available knowledge for IL + MS mixtures by the consideration of natural ions such as aminoacid – bases ones.

## 2. Materials and methods

### 2.1. Chemicals

The [bmim][glu] was synthesized through the synthesis of alkyylimidazolium hydroxide which is neutralized with glutamic acid as proposed by Fukumoto et al. [62], Fig. 2. In order to reduce the bromine content in the final product, the IL was cleaned with dichloromethane and anhydrous ether, therefore the addition of AgNO<sub>3</sub> to the wash liquid, occurred no precipitation of AgBr. The synthesized [bmim][glu] was dried under vacuum (<0.1 KPa) at 353 K, thus decreasing the water content as well as eliminating volatile compounds (dichloromethane, anhydrous ether and methyl imidazole). The water content of [bmim][glu] sample was determined by using the Karl Fisher titration (ZSD-2 type), with the water mass percent being lower than 10<sup>-4</sup>. The dried [bmim][glu] sample was analyzed by <sup>1</sup>H NMR (VarianXL-300) with the spectrum being in agreement with the literature [63]. The total peak integral in the <sup>1</sup>H NMR spectrum corresponds for [bmim][glu] to a nominal purity of about 99%.

The studied alkanols, isobutanol (mass fraction < 99%, Merck), 1-propanol (mass fraction ≥ 99.5%, Merck) and 1,2-propanediol (mass fraction ≥ 99.5%, Merck) were used as received without further purification. The specification of materials used in this study are reported in Table S1 (Supplementary Information).

### 2.2. Apparatus and procedure

Binary mixtures in the whole composition range, defined using mole fraction of [bmim][glu], *x*, were prepared freshly before each experiment, by weighing components on an analytical balance

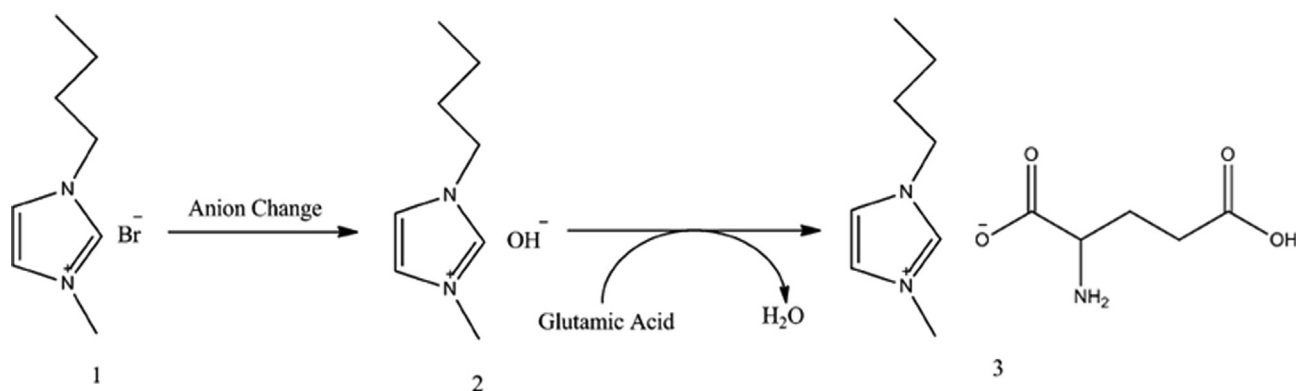


**Fig. 2.** Synthetic route for the production of [bmim][glu]. 1: [bmim] [Br], 2: [bmim] [OH], 3: [bmim] [glu]

**Table 1**

*In silico* predicted ecotoxicological properties for neat [bmim][glu] and [bmim][glu] + alkanols (1PRO or ISOBUT or 12PD) mixtures. (-) indicates nontoxic, (+) indicates toxic, (III) for acute oral toxicity indicates slightly toxic, {} values indicate the probability for each property. Results in bold indicate toxicity for the reported property.

Property	[bmim][glu]	[bmim][glu] + 1PRO	[bmim][glu] + ISOBUT	[bmim][glu] + 12PD
carcinogenicity	(-) {0.7857}	(-) {0.8286}	(-) {0.8714}	(-) {0.8857}
eye irritation	(-) {0.5953}	(-) {0.5967}	<b>(+) {0.5432}</b>	(-) {0.7561}
ames mutagenesis	(-) {0.7600}	(-) {0.7500}	(-) {0.8000}	(-) {0.7700}
biodegradation	(-) {0.5250}	<b>(+) {0.5250}</b>	<b>(+) {0.5750}</b>	<b>(+) {0.5750}</b>
crustacea aquatic toxicity	(-) {0.6000}	(-) {0.6621}	(-) {0.6652}	(-) {0.6952}
fish aquatic toxicity	(-) {0.6463}	(-) {0.8257}	(-) {0.7654}	(-) {0.8984}
acute oral toxicity	(III) {0.6673}	(III) {0.6624}	(III) {0.6663}	(III) {0.6579}
water solubility ( $\log S$ )	-1.935	-2.005	-2.116	-1.909

(Sartorius TE124S), and stored in airtight glass bottles. The expanded uncertainty in the mole fraction,  $U(x)$ , was estimated to be 0.0001. Samples were degassed (20 min) before each measurement using an ultrasound device (MISONIX Ultrasonic Liquid Processors).

Density,  $\rho$ , and speed of sound,  $u$ , were simultaneously determined by means of Anton Paar densitometer and sound analyzer (DSA 5000). Density measurements are based on the oscillating u-tube method. Viscosity-related errors are corrected by measuring the damping effect of the sample. The cells temperature was controlled through Peltier elements with the two integrated Pt100 platinum thermometers. Calibration was performed using degassed water and air, as the recommended procedure [64]. The experimental data allowed the calculation of excess molar volume,  $V^E$ , mixing isentropic compressibility,  $\Delta k_s$ , excess thermal expansion coefficient,  $\alpha_p^E$ , and mixing speed of sound,  $\Delta u$ , according to the equations reported in the [Supplementary Information](#). The analysis of the uncertainties of measurements with DSA 5000 equipment was recently reported by Wagner et al. [65]. Therefore, the uncertainties for all the experimental and calculated properties considered in this work are reported in Table S2 ([Supplementary Information](#)). The properties for pure compounds are reported in

Table S3 ([Supplementary Information](#)) whereas those for the mixtures are included in Tables S4 to S6 ([Supplementary Information](#)). The excess and mixing properties were fitted with mixture mole

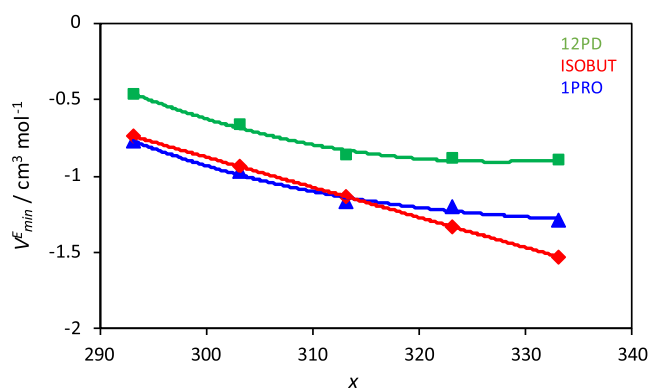


**Fig. 4.** Excess volume at minimum,  $V_{min}^E$ , for  $x$  [bmim][glu] +  $(1-x)$  {1PRO or ISOBUT or 12PD}, where  $x$  stands for mole fraction, as a function of temperature. Symbols indicate experimental results, lines indicate polynomial fits for guiding purposes.

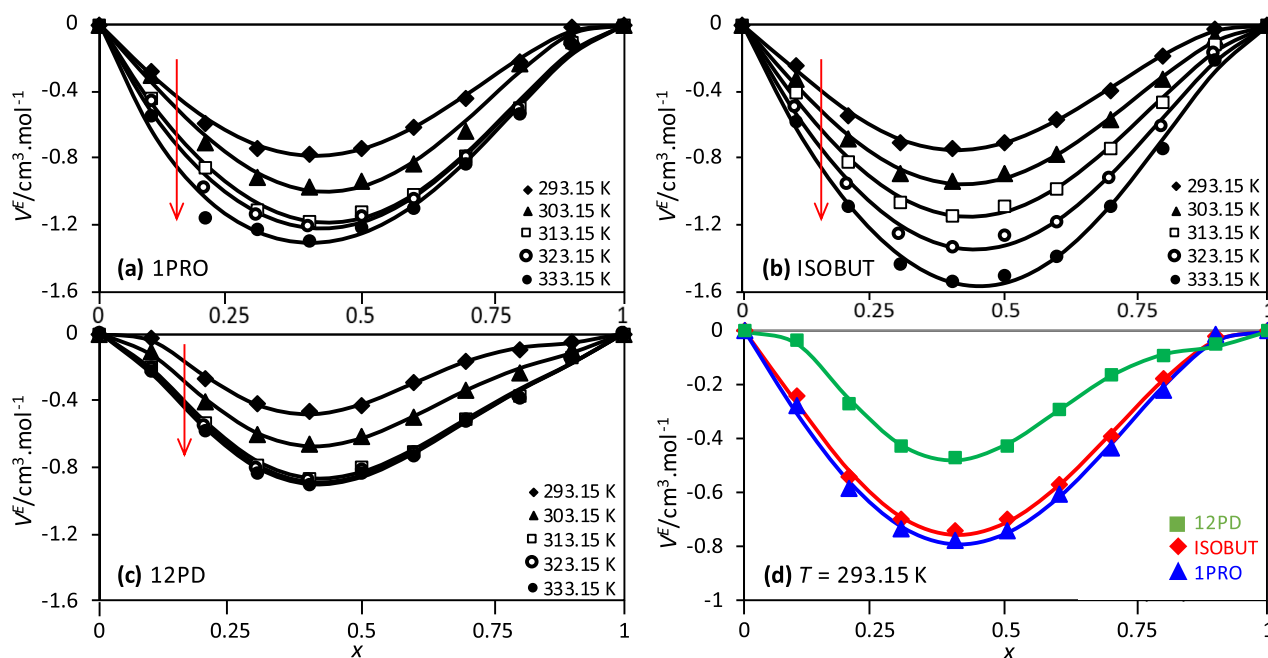


**Fig. 3.** Excess volume,  $V^E$ , for  $x$  [bmim][glu] +  $(1-x)$  {(a) 1PRO or (b) ISOBUT or (c) 12PD}, where  $x$  stands for mole fraction, as a function of temperature. In panel c, a comparison at 293.15 K is reported. Red arrows indicate increasing temperature. Symbols indicate experimental results, lines indicate fits to Redlick-Kister polynomial with coefficients reported in Table S7 ([Supplementary Information](#)). (For interpretation of the references to color in this figure legend, the reader is referred to the web version of this article.)

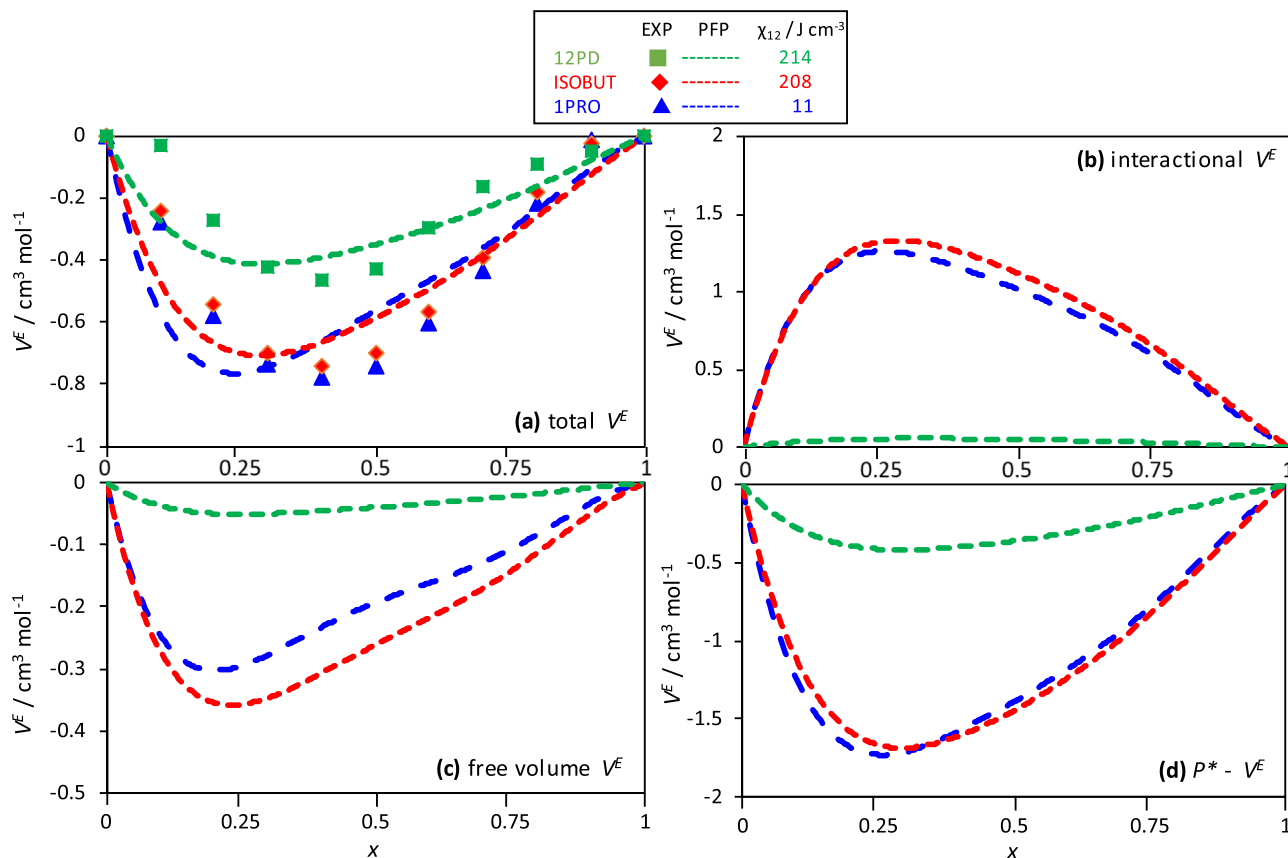


**Fig. 5.** Comparison of experimental, EXP, and Prigogine-Flory-Patterson, PFP, excess molar volume,  $V^E$ , for  $x$  [bmim][glu] +  $(1-x)$  {1PRO or ISOBUT or 12PD} mixtures, where  $x$  stand for mole fraction, at 293.15 K. Results in panels b to d show interactional, free volume and  $P^*$  PFP contributions to the total  $V^E$ . Symbols indicate experimental results, dashed lines indicate fits to PFP, with pure compounds properties as reported in Table S11 (Supplementary Information) and coefficients  $\chi_{12}$  reported on top of the Figure.

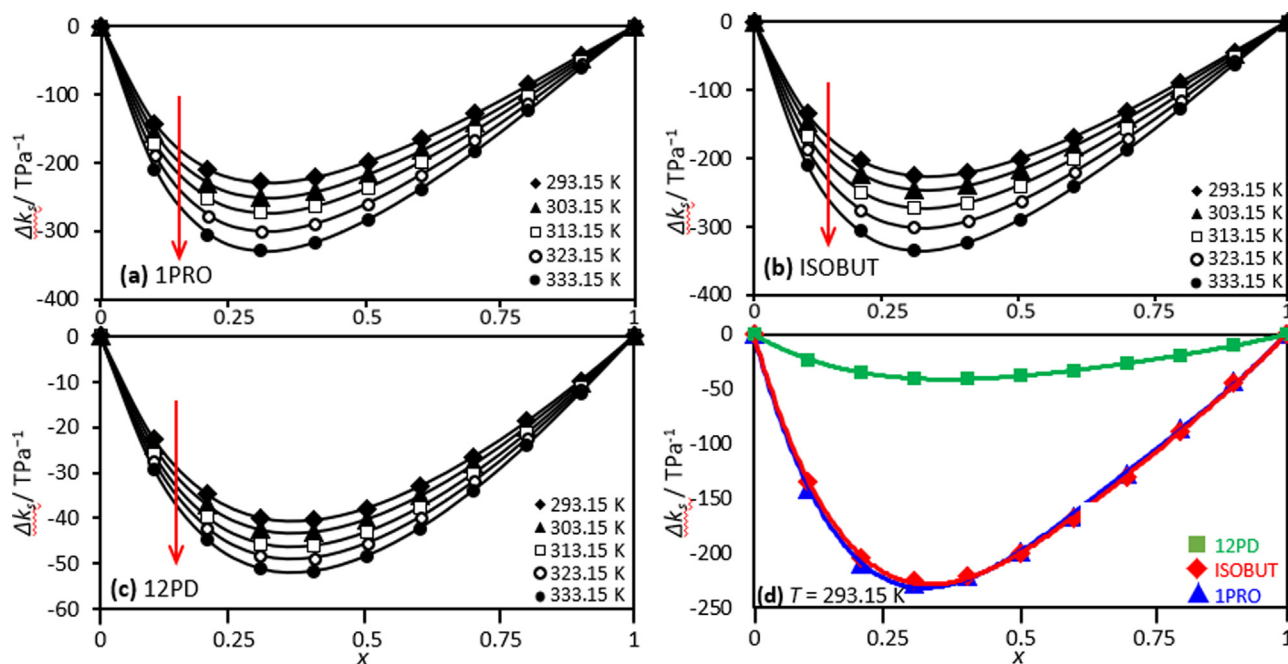


**Fig. 6.** Mixing isentropic compressibility,  $\Delta k_s$ , for  $x$  [bmim][glu] +  $(1-x)$  {1PRO or ISOBUT or 12PD}, where  $x$  stands for mole fraction, as a function of temperature. In panel d, a comparison at 293.15 K is reported. Red arrows indicate increasing temperature. Symbols indicate experimental results, lines indicate fits to Redlick-Kister polynomial with coefficients reported in Table S7 (Supplementary Information). (For interpretation of the references to color in this figure legend, the reader is referred to the web version of this article.)

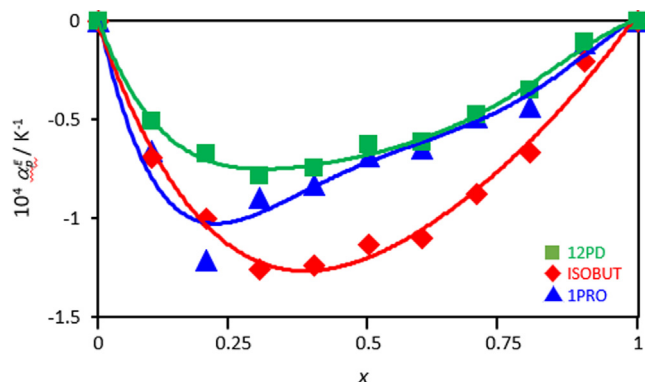


Fig. 7. Excess thermal expansion coefficient,  $\alpha_p^E$ , for  $x$  [bmim][glu] +  $(1-x)$  {1PRO or ISOBUT or 12PD}, where  $x$  stands for mole fraction, at 293.15 K. Symbols indicate experimental results, lines indicate fits to Redlich-Kister polynomial with coefficients reported in Table S7 (Supplementary Information).

fraction using Redlich-Kister polynomials, Table S7 (Supplementary Information). Likewise, for each  $i$  component in the mixture, the partial molar volume  $\bar{V}_i$ , the excess partial molar volume,  $\bar{V}_i^E$ , and the partial molar volume at infinite dilution,  $\bar{V}_i^{E,\infty}$ , were calculated (Table S8, Supplementary Information).

Additional analysis on the quality of measurements as well as on the purity of the pure substances was carried out by comparison of density and speed of sound with the available literature data [66–80], Table S3 (Supplementary Information), thus showing suitable agreement.

### 2.3. Ecotoxicological predictions

The available literature showed moderate toxicity and suitable biodegradability of AAILs [22–24]. Nevertheless, the scaling up of the considered fluids would require to study the toxicological and environmental (ecotoxicity) properties of the studied AAIL ([bmim][glu]) as well as their mixtures with the considered alkanols (1PRO, ISOBUT, 12PD). It is well-known the large cost of experimental determination of ecotoxicological properties, both in time and resources [81], thus the *in-silico* prediction is considered as a reliable and more efficient approach, which may led to at least an initial estimation of the most relevant properties for novel compounds. For the systems considered in this work, an *in-silico* approach was considered using ADMETSAR 2.0 software tool [82]. ADMETSAR 2.0 uses machine learning method for predicting ecotoxicological properties of chemicals from the available databases. The large database considered for training of ADMETSAR 2.0, as well as the strength of the considered predictive models have allowed to develop reliable predictions for many different compounds [81], even for ILs [83,84]. Properties relevant to analyze the environmental fate and toxicological properties of the considered AAIL and the alkanol mixtures were selected and predicted. SMILES were created from the optimized structures of each system and used as input files for the ecotoxicological predictions.

### 2.4. Molecular modelling

Two different theoretical approaches were considered to study the behavior and properties of [bmim][glu] + alkanol liquid mixtures: *i*) quantum chemistry methods based on the Density Functional Theory (DFT) and *ii*) classical molecular dynamics simulations (MD).

DFT calculations were carried out using the ORCA program (version 4.2.1) [85]. The DFT studies were carried out on minimal clus-

ters to analysed anion – cation and IL – alkanol interactions. Therefore, for these purposes, the following systems were considered: *i*) [bmim] : [glu] 1:1 pair, and *ii*) [bmim] : [glu] : alkanol 1:1:1 clusters. For all the cases, the main possible interaction sites were considered. The structures of the considered clusters were subjected to geometry optimizations at B3LYP [86–88] plus 6–311++G(d,p) theoretical level, including van der Waals interactions as treated using Grimme's method (DFT-D3) [89]. The interaction energies,  $\Delta E$ , were calculated for each cluster as the energy difference of the cluster energy and the sum of the energies of the corresponding monomers as in equation (1).

$$\Delta E = E_{\text{bmim\_glu+1PRO/ISOBUT/12PD}} - E_{\text{bmim}} - E_{\text{glu}} - E_{\text{1PRO/ISOBUT/12PD}} \quad (1)$$

The Basis Set Superposition Error (BSSE) was corrected using the counterpoise method [90]. The atomic charges were calculated for optimized structures using the ChelpG method [91]. The topological properties of the studied clusters were analyzed according to the Quantum Theory of Atoms in a Molecule (QTAIM [92]) and the Reduced density Gradient method (RDG [93]) using Multiwfn software (version 3.6) [94].

MD simulations for [bmim][glu] + alkanol liquid mixtures in the whole composition range were carried out using MDynaMix v.5.2 [95]. The initial cubic simulation boxes for the compositions, number of molecules and dimensions, as reported in Table S9 (Supplementary Information), were built using Packmol [96] program. The forcefields applied for the involved molecules are reported in Table S10 (Supplementary Information). The forcefield parameters were obtained as a combination of parameters derived from SwissParam database (Merck Molecular Force Field [97]) and atomic charges inferred in this work from ChelpG charges obtained from DFT simulations of isolated monomers (1PRO, ISOBUT or 12PD) or of [bmim]-[glu] pairs for the ions in the considered IL. The force

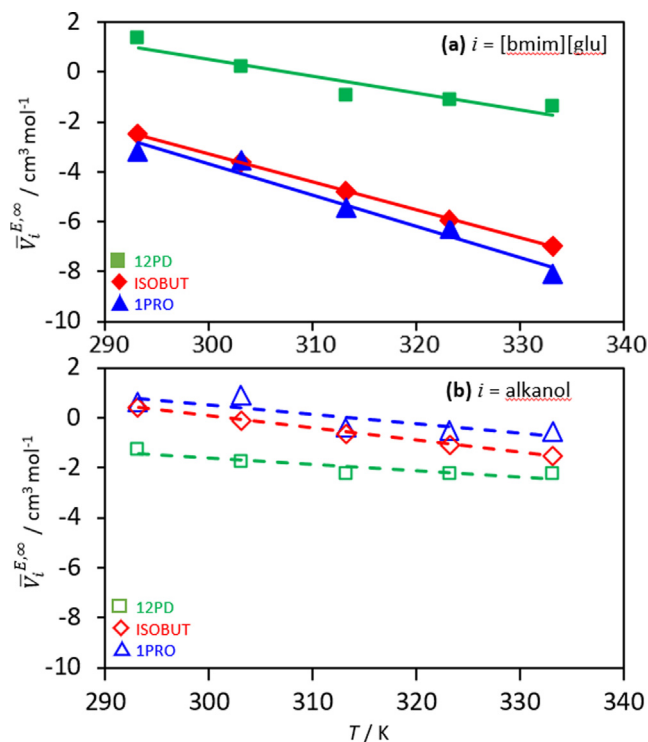


Fig. 8. Excess partial molar volume at infinite dilution for  $i$  compound for  $x$  [bmim][glu] +  $(1-x)$  {1PRO or ISOBUT or 12PD}, where  $x$  stands for mole fraction, as a function of temperature,  $T$ . Panel a shows results for [bmim][glu] (i.e.  $x \rightarrow 0$ ) and panel b results for the corresponding alkanol ( $x \rightarrow 1$ ). Symbols indicate experimental results, lines indicate polynomial fits for guiding purposes.

**Table 2**

Counterpoise corrected binding energies,  $\Delta E$ , and total ChelpG charges,  $Q$ , ([bmim][glu]/(1PRO, ISOBUT or 12PD). Values for the reported molecular clusters (IL + 1PRO/ISOBUT/12PD, 1:1 pairs) obtained from optimized geometries at B3LYP-D3/6-311++G(d,p) theoretical level. Parenthesized values in  $\Delta E$  for clusters containing alkanols show  $\Delta E$  subtracting the corresponding interaction energy for the [bmim][glu] pairs (site #1). Sites are defined as in Fig. S1 (Supplementary Information).

Site	$\Delta E / \text{kJ mol}^{-1}$			
	[bmim][glu]	[bmim][glu] + 1PRO	[bmim][glu] + ISOBUT	[bmim][glu] + 12PD
#1	-398.6	-429.2 (-30.6)	-431.6 (-33.0)	-429.4 (-30.8)
#2	-354.1	-432.7 (-34.1)	-439.6 (-41.0)	-439.1 (-40.5)
#3	-359.8	-425.6 (-27.0)	-468.4 (-69.8)	-450.7 (-52.1)
#4		-461.9 (-63.3)	-443.5 (-44.9)	-483.4 (-84.8)
$q$				
#1	0.8895/-0.8895	0.9125/-0.9022/-0.0103	0.8794/-0.9038/0.0244	0.8797/-0.8883/0.0085
#2	0.8990/-0.8990	0.9216/-0.9054/-0.0162	0.8883/-0.8701/-0.0182	0.8589/-0.8366/-0.0223
#3	0.9183/-0.9183	0.8736/-0.8139/-0.0597	0.8540/-0.9340/0.0800	0.8633/-0.7694/-0.0938
#4		0.8420/-0.8767/0.0347	0.8734/-0.7186/-0.1548	0.7912/-0.7799/-0.0113

**Table 3**

QTAIM analysis: (3,-1) bond critical points (black) and (3,+1) ring critical points (bold). Values reported show electron density,  $\rho_e$ , at the corresponding critical point and the  $\nabla^2\rho_e$  (a.u.) for the reported molecular clusters. Critical points (CPs) defined as in Fig. S2 (Supplementary Information).

[bmim][glu]				[bmim][glu] + ISOBUT					
Site	CPs	$\rho_e / \text{a.u.}$	$\nabla^2\rho_e / \text{a.u.}$	Site	CPs	$\rho_e / \text{a.u.}$	$\nabla^2\rho_e / \text{a.u.}$		
#1	75	0.0393	0.1192	#1	72	0.0213	0.0870		
	76	0.0210	0.0762		91	0.0280	0.0948		
	<b>80</b>	<b>0.0079</b>	<b>0.0351</b>		92	0.0179	0.0656		
					97	0.0192	0.0708		
			140		0.0144	0.0517			
			<b>70</b>		<b>0.0206</b>	<b>0.1117</b>			
			<b>90</b>		<b>0.0173</b>	<b>0.0705</b>			
#2	69	0.0266	0.0888		#2	76	0.0242	0.0936	
	71	0.0397	0.1215			87	0.0125	0.0400	
	<b>70</b>	<b>0.0069</b>	<b>0.0301</b>			121	0.0439	0.1254	
						122	0.0197	0.0663	
			<b>81</b>			<b>0.0108</b>	0.0494		
			<b>125</b>	<b>0.0079</b>		0.0349			
#3	77	0.0240	0.0839	#3		80	0.0205	0.0865	
	82	0.0375	0.1147			116	0.0422	0.1347	
	72	0.0061	0.0244			131	0.0235	0.0800	
	<b>76</b>	<b>0.0068</b>	<b>0.0303</b>			<b>123</b>	<b>0.0174</b>	<b>0.0696</b>	
			#4			93	0.0401	0.0973	
						117	0.0413	0.1222	
					119	0.0203	0.0718		
					<b>121</b>	<b>0.0078</b>	<b>0.0348</b>		
[bmim][glu] + 1PRO					[bmim][glu] + 12PD				
#1	67	0.0210	0.0859		#1	74	0.0211	0.0868	
	92	0.0227	0.0801			88	0.0313	0.1029	
	94	0.0216	0.0772			92	0.0202	0.0741	
	<b>66</b>	<b>0.0204</b>	<b>0.1098</b>	131		0.0185	0.0654		
			<b>72</b>	<b>0.0204</b>		<b>0.1115</b>			
#2	90	0.0211	0.0869	#2		105	0.0373	0.1134	
	115	0.0420	0.1207			107	0.0237	0.0867	
	116	0.0251	0.0907			<b>76</b>	<b>0.0190</b>	<b>0.0984</b>	
	<b>89</b>	<b>0.0205</b>	<b>0.1113</b>						
#3	98	0.0342	0.1091			#3	77	0.0202	0.0863
	99	0.0179	0.0635				105	0.0432	0.1455
	<b>73</b>	<b>0.0203</b>	<b>0.1099</b>				108	0.0198	0.0660
					111		0.0487	0.1358	
			116		0.0187		0.0658		
			<b>78</b>		<b>0.0199</b>		<b>0.1049</b>		
#4	79	0.0099	0.0281		#4		80	0.0376	0.0948
	86	0.0274	0.0947				97	0.0190	0.0654
	122	0.0095	0.0358	103			0.0362	0.1255	
	<b>66</b>	<b>0.0196</b>	<b>0.1028</b>	114			0.0379	0.1160	
			122	0.0228			0.0783		
			<b>75</b>	<b>0.0080</b>			<b>0.0268</b>		
			<b>92</b>	<b>0.0061</b>		<b>0.0250</b>			
			<b>119</b>	<b>0.0068</b>		<b>0.0301</b>			

field parameterizations were validated by comparison of experimental and simulated densities in the whole composition range, Figure S4 (Supplementary Information), showing excellent agreement, with deviation lower than 3% in the whole composition

range for all the studied mixtures. MD simulations were carried out in a two steps procedure: i) initial simulation boxes were subjected to NVT simulations at 313 K for 1 ns and ii) followed by NPT simulations at 313 K and 1 bar for 40 ns, where the initial 20 ns

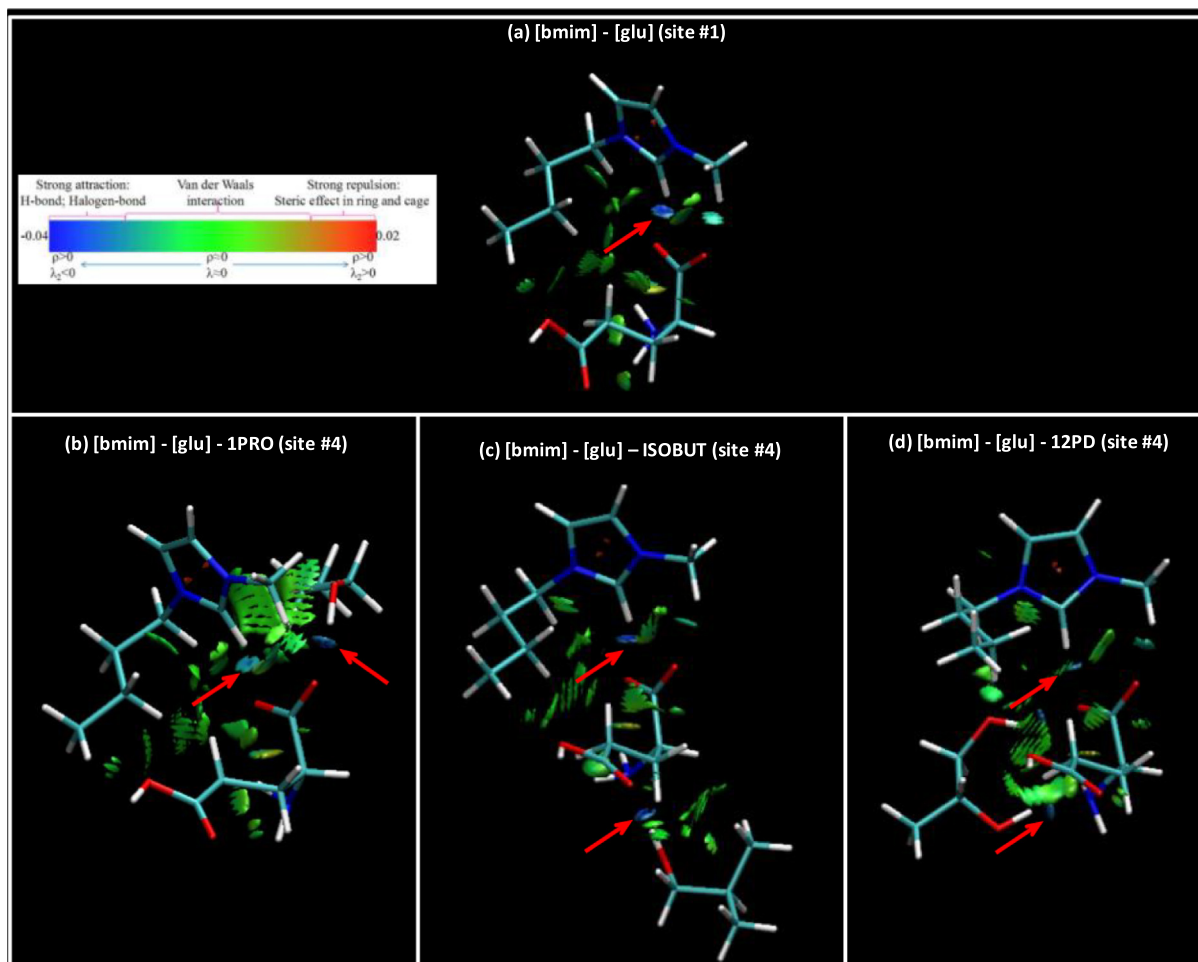


**Fig. 9.** RDG analysis of (a) [bmim] – [glu] and (b,c,d) [bmim] – [glu] – alkanol (1PRO, ISOBUT or 12PD). Interaction sites labelling as in Figure S1 (Supplementary Information). Red arrows indicate the most relevant features (hydrogen bonding sites). (For interpretation of the references to color in this figure legend, the reader is referred to the web version of this article.)

were considered for equilibration purposes, assured through the constancy of system potential energy, and the remaining 20 ns for production and analysis. The systems temperature and pressure were controlled with Nose-Hoover method, with 0.1 and 0.5 ps coupling times for temperature and pressure, respectively. Tuckerman-Berne double time step algorithm [98] was considered for solving the equations of motion, with 1 and 0.1 fs for long- and short-time steps. The Ewald method [99] (15 Å for cut-off radius) was used for treating electrostatic interactions. As the Lennard-Jones potential was considered, Table S10 (Supplementary Information), a 15 Å cut-off was applied and cross terms were calculated using Lorentz-Berthelot mixing rules.

### 3. Results and discussion

#### 3.1. Toxicity and ecotoxicity prediction

The predicted ecotoxicological properties of neat [bmim][glu] AAILs as reported in Table 1 show that this AAIL is non-toxic, non-carcinogenic and non-mutagenic, with high probability for all these relevant properties. Likewise, it is water soluble and non-toxic for water living-things. It may be classified as slightly toxic (type III) in terms of oral toxicity. Regarding the biodegradability, although it is classified as biodegradable, the corresponding

probability is only 52 %, thus it is moderately biodegradable, which may constitute the main problem for this AAIL.

The ecotoxicological properties of [bmim][glu] stands on its water solubility, although it is non-toxic for aquatic organisms. The addition of alkanols to [bmim][glu] leads to some changes in toxicological properties. The main change stands on the poorer biodegradation when compared with the neat AAILs, although this was also the main problem of the neat AAIL. On the contrary the remaining properties are slightly improved with the addition of the alkanol, the probabilities for non-toxic effects increase with the alkanol for the studied compounds (1PRO, ISOBUT and 12PD), thus making safer the use of [bmim][glu] when mixed with alkanols. Therefore, the considered AAIL + alkanol mixtures can be considered not only for tuning the AAILs physicochemical properties but also for improving the ecotoxicological profile of the ionic liquid, with the exception of biodegradation.

#### 3.2. Experimental properties: Thermophysics

The systems [bmim][glu] + alkanols (1PRO or ISOBUT or 12PD) are experimentally characterized in the whole composition range in the 293.15 to 333.15 K temperature range. The experimental density and speed of sound data, as well as the derived excess and mixing properties, are reported in Tables S4 to S6 (Supplementary Information). Excess and mixing properties were successfully fitted

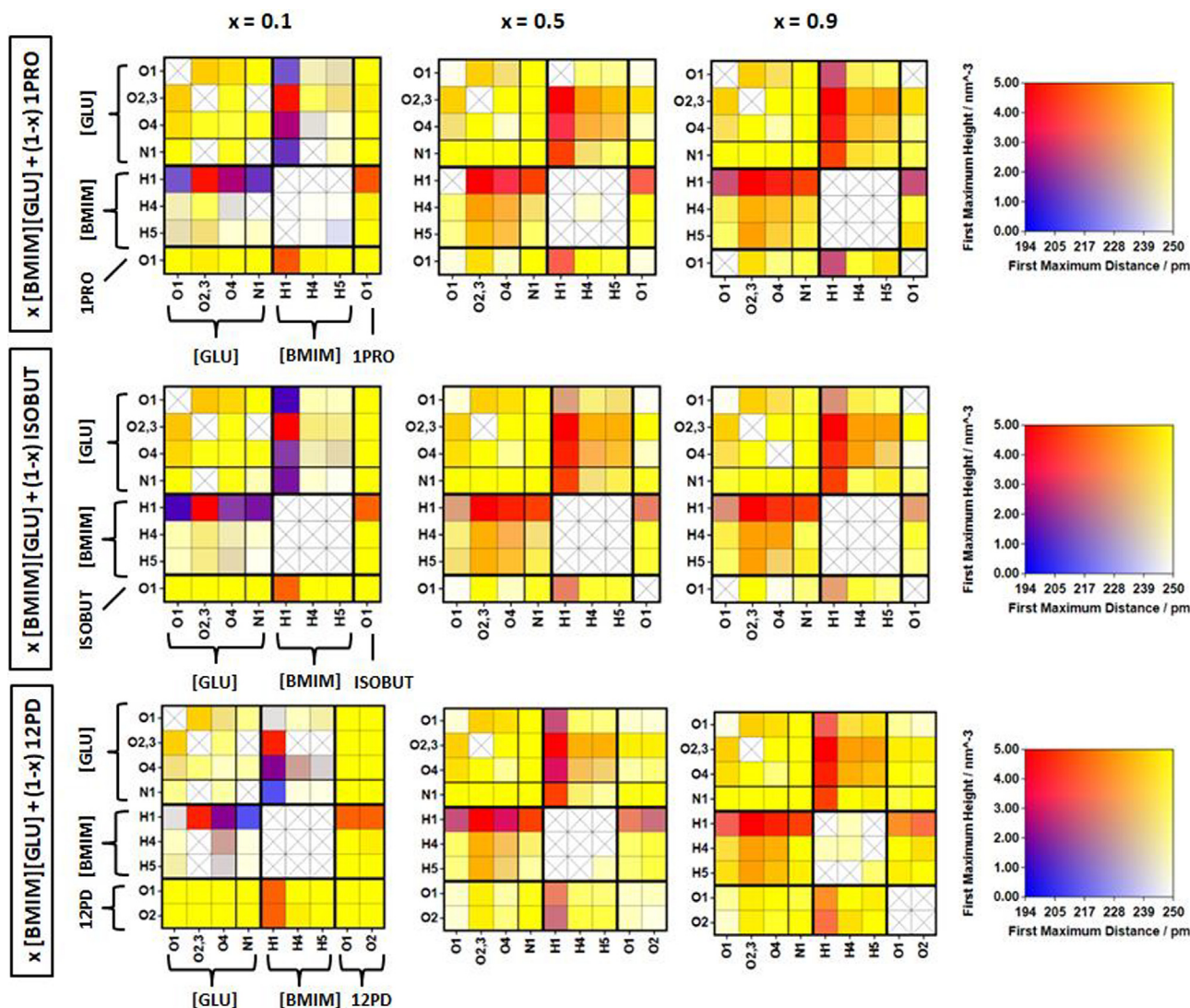


**Fig. 10.** Connection matrix analysis of  $x$  [BMIM][GLU] +  $(1-x)$  1PRO/ISOBUT/12PD. Rows represent hydrogen bond acceptors, and columns stand for hydrogen bond donors. The color in each square represents both the intensity and distance of the first maximum in the corresponding RDF (for color scale, see the right-hand side).

to Redlich – Kister polynomials as reported in Table S7 (Supplementary Information).

The results for  $V^E$  are reported in Fig. 3 for the three considered alkanols in the studied temperature range, reporting negative values for all the studied mixtures, compositions and temperatures. The behavior of  $V^E$  points to stronger attractive interactions between the unlike molecules than the like ones. Likewise, the variation of intermolecular forces and the molecular packing (resulting from difference in the size and shape of the molecules of mixture components) upon mixing is on the root of the negative sign of  $V^E$ . The  $V^E$  curves reported in Fig. 3 are not symmetrical (i.e. not centered at equimolar compositions), the  $V^E$  minimum value occurs at about  $x = 0.4$  ( $x$  stands for [bmim][glu] mole fraction) for all mentioned binary mixtures. The steric effects on  $V^E$  may be also considered having in mind the molar volumes for pure compounds, thus being 223.57, 74.67, 92.42, and 73.43  $\text{cm}^3 \text{mol}^{-1}$  at 293.15 K (Table S8, Supplementary Information) for [bmim][Glu], 1PRO, ISOBUT, and 12PD, respectively. The value of molar volume for [bmim][glu] is remarkably larger than for the considered alkanols. The large difference in molar volumes between mixture components may lead to large steric effects with liquids structuring characterized by clathrate – like structuring, with the

alkanol molecules filling the interstices provided by [bmim][glu] arrangements, thus leading to negative values of the  $V^E$ . A comparable phenomenon has been previously observed in similar systems containing ILs and molecular solvents [100,101]. The type of alkanol involved in the liquid mixture has a large effect on  $V^E$ , Fig. 3d, thus following the sequence 1PRO < ISOBUT << 12PD. This behavior can be justified because of the larger extension of self-hydrogen bonding in 12PD considering the two available hydroxyl groups per molecule, in comparison with a single one for 1PRO and ISOBUT, thus the mixing of 12PD with the IL leads to larger disruption of self-aggregation (an expansive contribution to the total volume), i.e. lower (in absolute value)  $V^E$ . The effect of the type of alkyl chain in the  $V^E$  is minor, although mixtures with ISOBUT show slightly (in absolute value) lower  $V^E$  than for 1PRO, which can be attributed to a steric effect caused by the bulkiest size of the ISOBUT molecules. Nevertheless, the main effect stands on the number of available hydroxyl groups which are prone to develop hydrogen bonding.

The increasing temperature leads to larger (in absolute value)  $V^E$ , which agrees with previous literature studies [102], Fig. 3 and Fig. 4. The variation of  $V^E$  with temperature is not linear, results in Fig. 4 show the temperature effect on  $V^E$  at minima,  $V_{min}^E$ , which

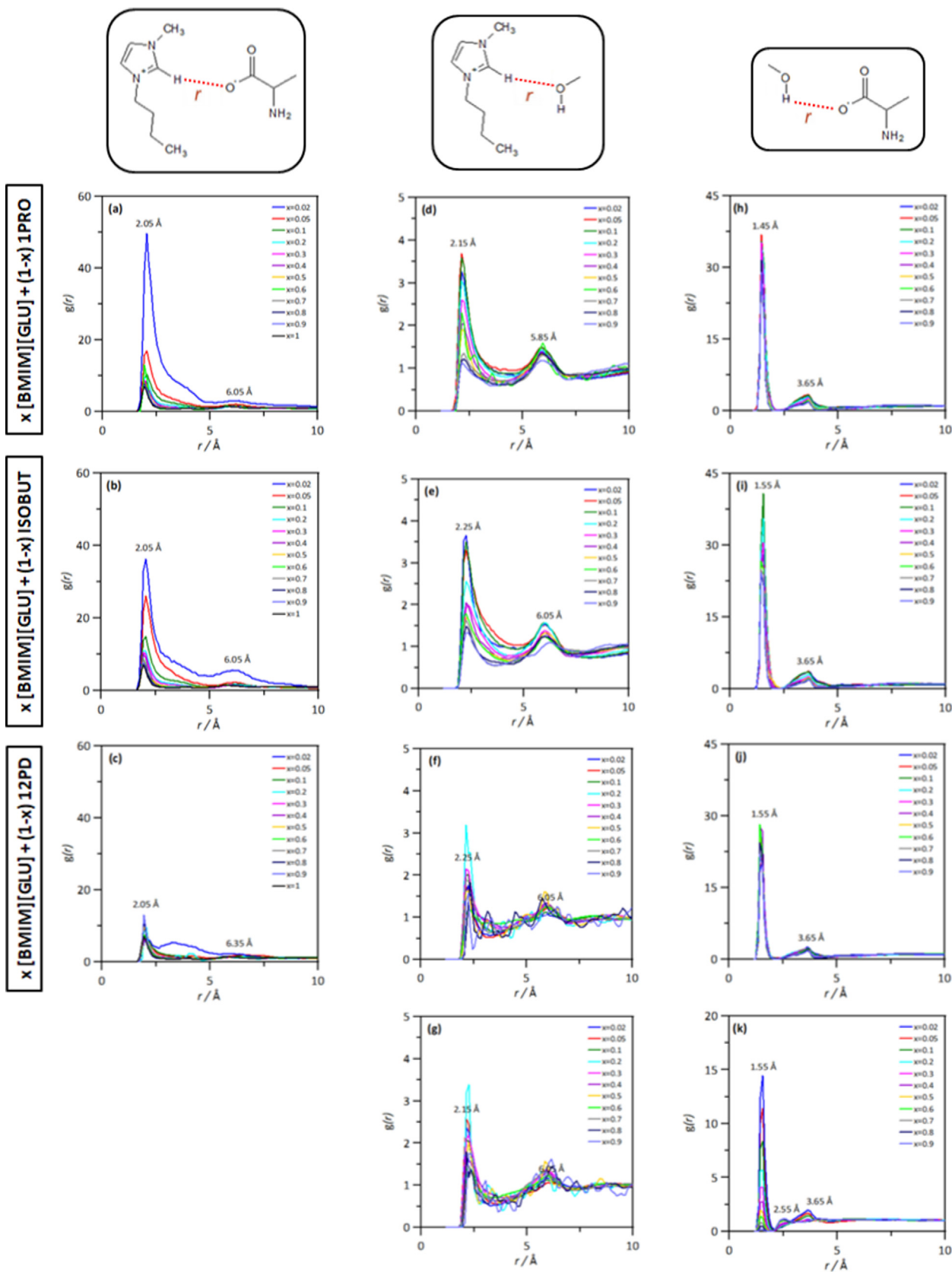
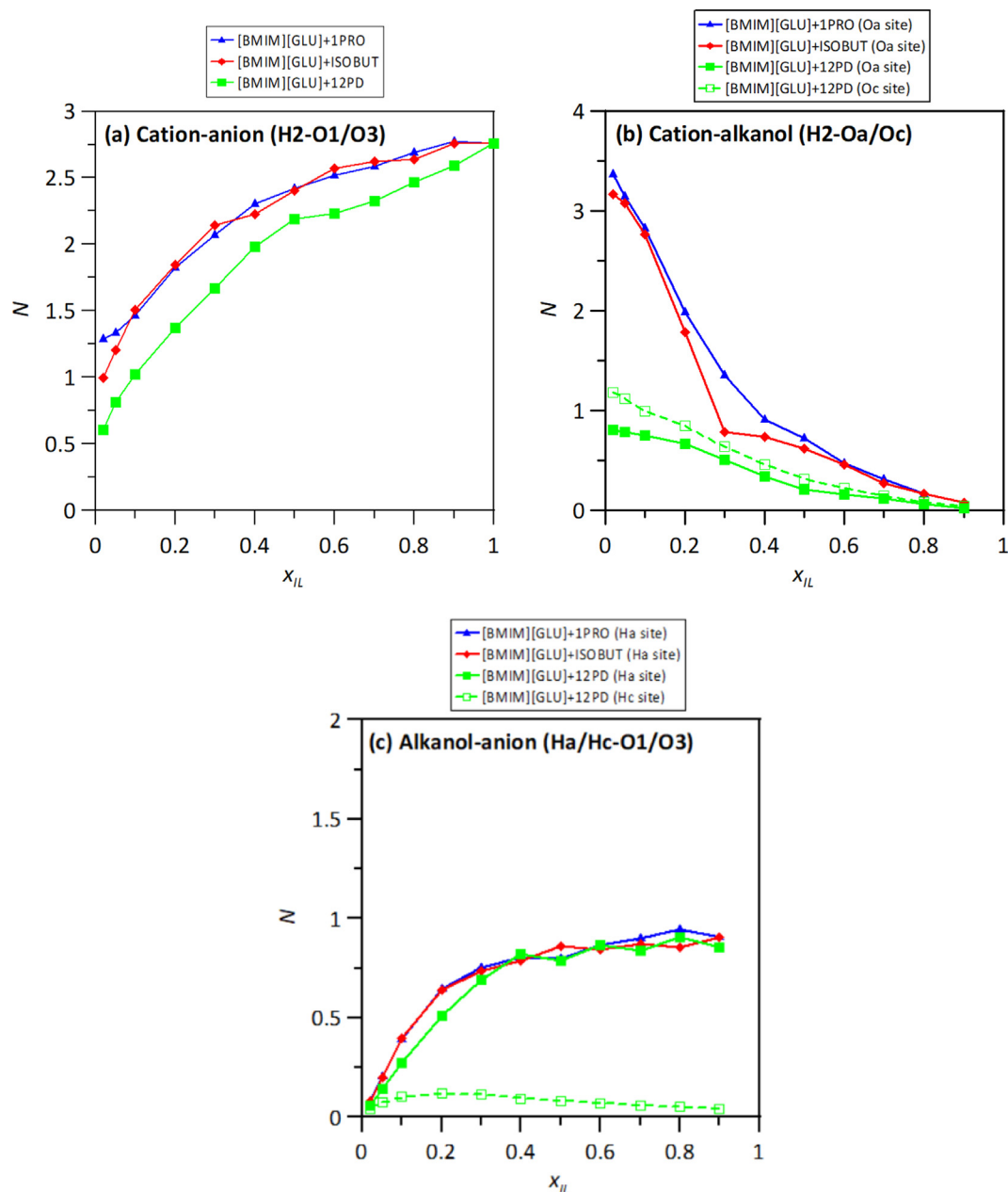


Fig. 11. Site-site radial distribution functions,  $g(r)$ , for cation-anion, cation-alkanol and anion-alkanol sites in  $x$  [BMIM][GLU] +  $(1-x)$  1PRO/ISOBUT/12PD,  $x$  stands for mole fraction, at 313 K and 0.1 MPa.



**Fig. 12.** Solvation numbers,  $N$ , obtained from the integration of radial distribution functions reported in Fig. 11, corresponding to the first solvation sphere, defined as the first minimum in the corresponding radial distribution function in  $x$  [BMIM][GLU] +  $(1-x)$  1PRO/ISOBUT/12PD,  $x$  stands for mole fraction, at 313 K and 0.1 MPa. Symbols indicate simulation results, lines are included for guiding purposes.

for 1PRO and 12PD shows a non-linear (in absolute value) increase, with lower changes for temperatures larger than 313.15 K, whereas for ISOBUT mixtures the decrease is almost linear.

Additional molecular – level information may be extracted from the measured  $V^E$  through the modelling of this property using the Prigogine-Flory-Patterson (PFP) [103]. The experimental  $V^E$  values were fitted through the  $\chi_{12}$  PFP interaction parameter, results in Fig. 5a show moderate fitting ability of PFP model. The main problem of PFP model stands on the prediction of the minima for the  $V^E$  vs mole fraction curves, which experimentally appears at roughly 0.4 IL mole fraction for all the studied alkanols and temperatures, it is predicted at 0.2 from PFP model. This difficulties in the prediction of the  $V^E$  stand on the large differences between the properties of pure compounds, e.g. the isothermal compressibility at 293.15 K

for [bmim][glu] is 0.218 GPa<sup>-1</sup> whereas for 1PRO is 1.007 GPa<sup>-1</sup>, with similar differences for properties such as density or thermal expansion coefficients (Table S11, Supplementary Information). Nevertheless, PFP model is able to fit the effect of alkanols on mixture properties, with remarkably lower  $V^E$  values for 12PD systems. The  $\chi_{12}$  PFP interaction parameter is very similar both for 1PRO and ISOBUT whereas it is remarkably lower for 12PD. The PFP model divides  $V^E$  into three different contribution considering different molecular effects: interactional, free volume and  $P^*$  terms. The PFP interactional contribution, Fig. 5b, is positive in the whole composition range, being larger for 1PRO / ISOBUT than for 12PD, which is close to null. This effect confirms the prevailing role of IL – alkanol through the available alkanol hydroxyl sites. The free volume terms, Fig. 5c, are largely negative for 1PRO and ISOBUT

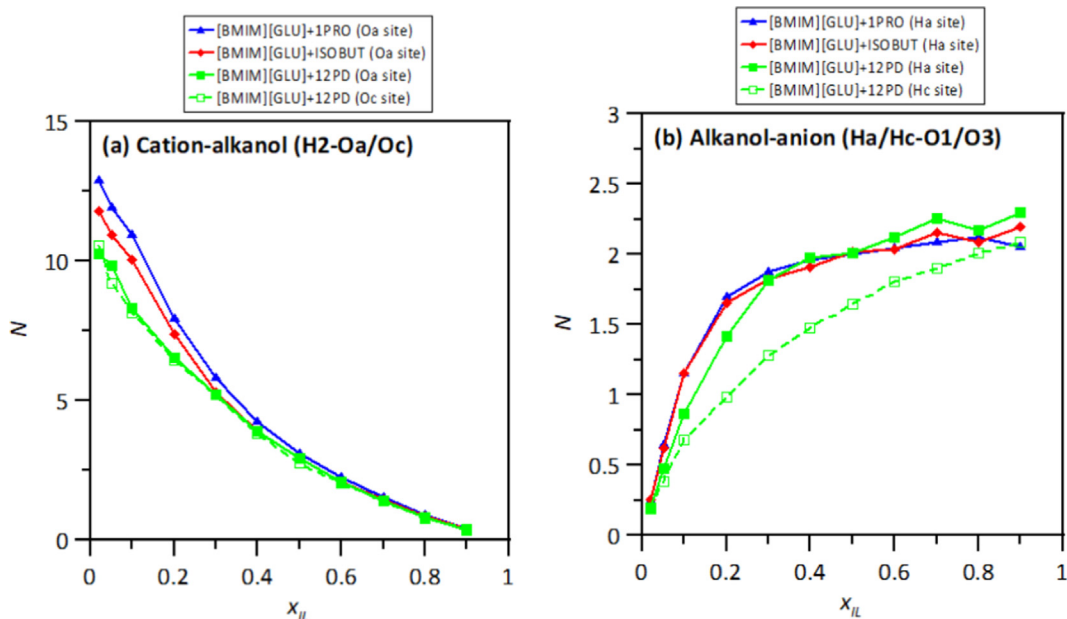


**Fig. 13.** Solvation numbers,  $N$ , obtained from the integration of radial distribution functions reported in Fig. 11, corresponding to the second solvation sphere, defined as the second minimum in the corresponding radial distribution function in  $x$  [BMIM][GLU] +  $(1-x)$  1PRO/ISOBUT/12PD,  $x$  stands for mole fraction, at 313 K and 0.1 MPa. Symbols indicate simulation results, lines are included for guiding purposes.

and remarkably smaller (in absolute value) for 12PD, which is caused by the lower differences among the volumetric properties of 12PD and the IL in comparison with 1PRO and ISOBUT (Table S11, Supplementary Information). Analogous behaviour is inferred for the  $P^*$  contribution, Fig. 5d. Therefore, the  $V^E$  for the studied mixtures is caused both by the development of IL – alkanol heteroassociation as well as for the large differences between the volumetric properties of the involved pure compounds, i.e. steric effects and association on the roots of the mixture's behaviour, with large effects on the number of available hydroxyl sites in the alkanol molecules.

The behaviour of  $\Delta k_s$  is reported in Fig. 6, being analogous to that for  $V^E$ . The  $\Delta k_s$  are negative for the three considered alkanol mixtures but remarkably larger for 1PRO and ISOBUT than for 12PD, i.e. 1PRO and ISOBUT mixtures suffers remarkably larger changes in compressibility upon mixing than 12PD ones. This effect can be justified by the larger  $V^E$  for 1PRO and ISOBUT mixtures, caused by the large differences among the volumetric properties of the IL and these alkanols. Therefore, a proper fitting upon mixing is allowed thus leading to less compressible fluids in comparison with pure solvents, especially when considering the large compressibility of 1PRO and ISOBUT (Table S11, Supplementary Information) in comparison with the IL, and thus being minor differences for 12PD. Analogous results are inferred for  $\alpha_p^E$ , Fig. 7, which confirms (in absolute) larger values for ISOBUT mixtures, i.e. caused by the bulkiest size of the alkanol molecule, but confirming the relevance of steric effects on the properties of these mixtures leading to less compressible fluids upon mixing. The partial molar volume properties are reported in Table S8 (Supplementary Information). It should be remarked the large differences among the properties of IL and the corresponding alkanols, with larger molar volumes and partial molar volumes for the IL. The partial molar volumes at infinite dilution  $\bar{V}_i^{-\infty}$ , quantifying the fitting of isolated molecules surrounded by the cosolvent, are also larger for IL than for the alkanol, and the derived  $\bar{V}_i^{-E,\infty}$  are mostly negative, with the exception of IL in 12PD at the lower temperatures. The reported  $\bar{V}_i^{-E,\infty}$ , Fig. 8, are (in absolute value) larger for [bmim]

[glu] than for the alkanols, with the exception of 12PD, showing that the IL is able to fit into the alkanol liquid structuring with more efficiency than vice versa, because the large degree of packing in the IL, as confirmed by its low compressibility (Table S11, Supplementary Information). In the case of 12PD, the positive  $\bar{V}_i^{-E,\infty}$  for the IL at low temperatures and the lower values in comparison with 1PRO and ISOBUT, indicates that the high degree of self-association between alkanol molecules hinders a proper packing of IL ions, thus leading to an expansive contribution, Fig. 8a. This is confirmed by the (in absolute value) larger  $\bar{V}_i^{-E,\infty}$  for 12PD in the IL in comparison with 1PRO and ISOBUT, Fig. 8b, as the effect of strong self-association for 12PD because of the presence of two hydroxyl molecules vanishes when infinitely diluted in the IL but these two hydroxyl groups are able to develop hydrogen bonding in larger extension with the IL through hydrogen bonding. The temperature evolution of  $\bar{V}_i^{-E,\infty}$  is linear for all the studied mixtures, thus showing how the steric effects are reinforced upon heating by the increase of molecular mobility and the size and extension of available space for proper molecular fitting into the cosolvent structuring.

### 3.3. Molecular modelling: DFT

The properties of [bmim][glu] ion pair were studied using DFT approach, the anion – cation dimer was optimized and the  $\Delta E$  was calculated. The [bmim] cation has two main types of sites through which it may develop interactions (i.e. possible hydrogen bonding) with the [glu] anion, i) the CH(2) site (placed in between the two N atoms of the imidazolium ring) and ii) the CH(1) sites in the imidazolium ring, Fig. 1. Therefore, three interaction sites are considered for [bmim] – [glu] pairs, Figure S1 (Supplementary Information): carboxylate group of [glu] anion in the vicinity of i) CH(2) (site #1) or of ii) CH(1) (sites #2 and #3). The  $\Delta E$  values are reported in. For the three considered [bmim] – [glu] interaction sites very large  $\Delta E$  are inferred, probing strong interactions, although site #1 (CH(2) in imidazolium) shows larger  $\Delta E$  in comparison with interactions through CH(1) imidazolium sites. The calculated

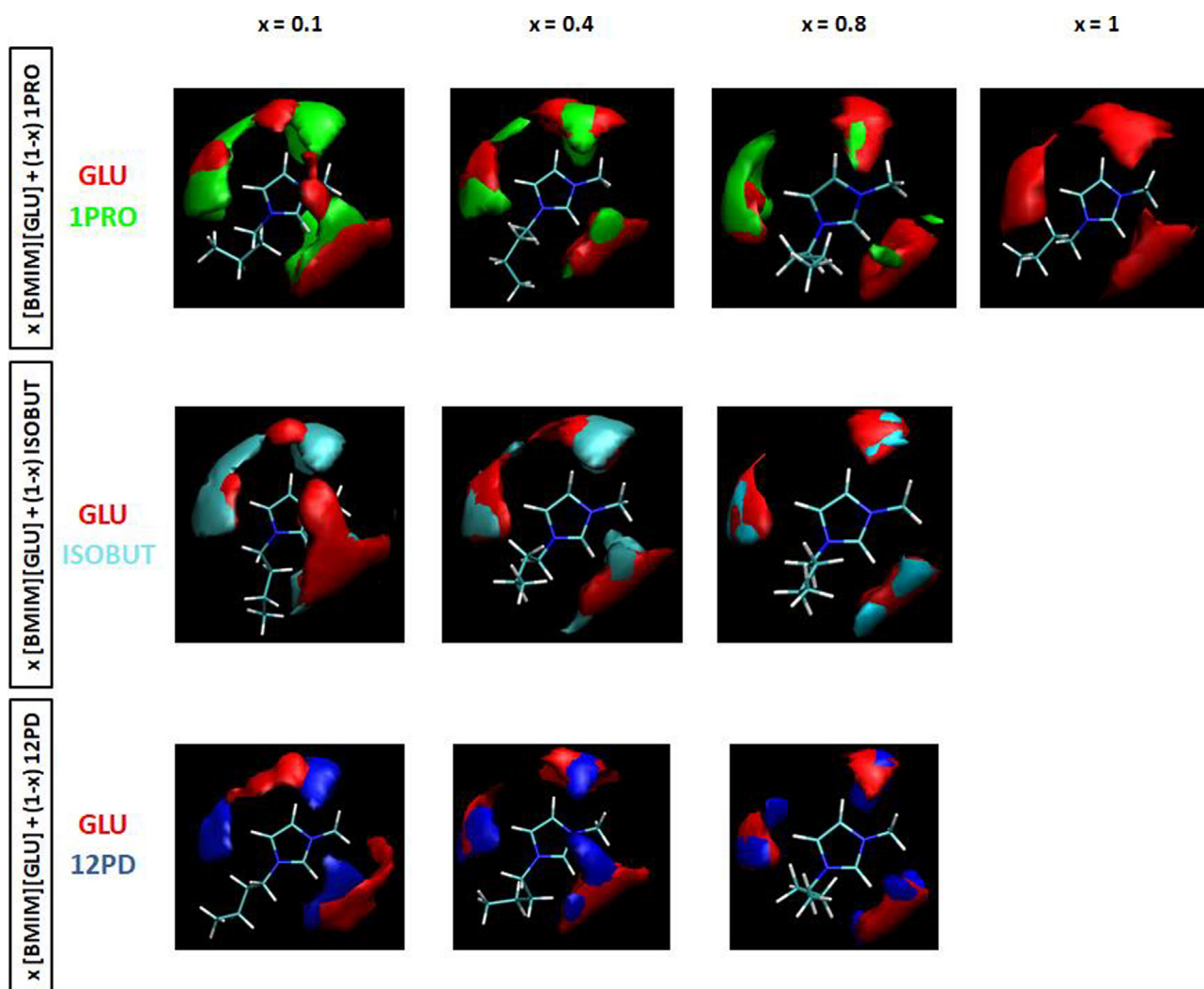
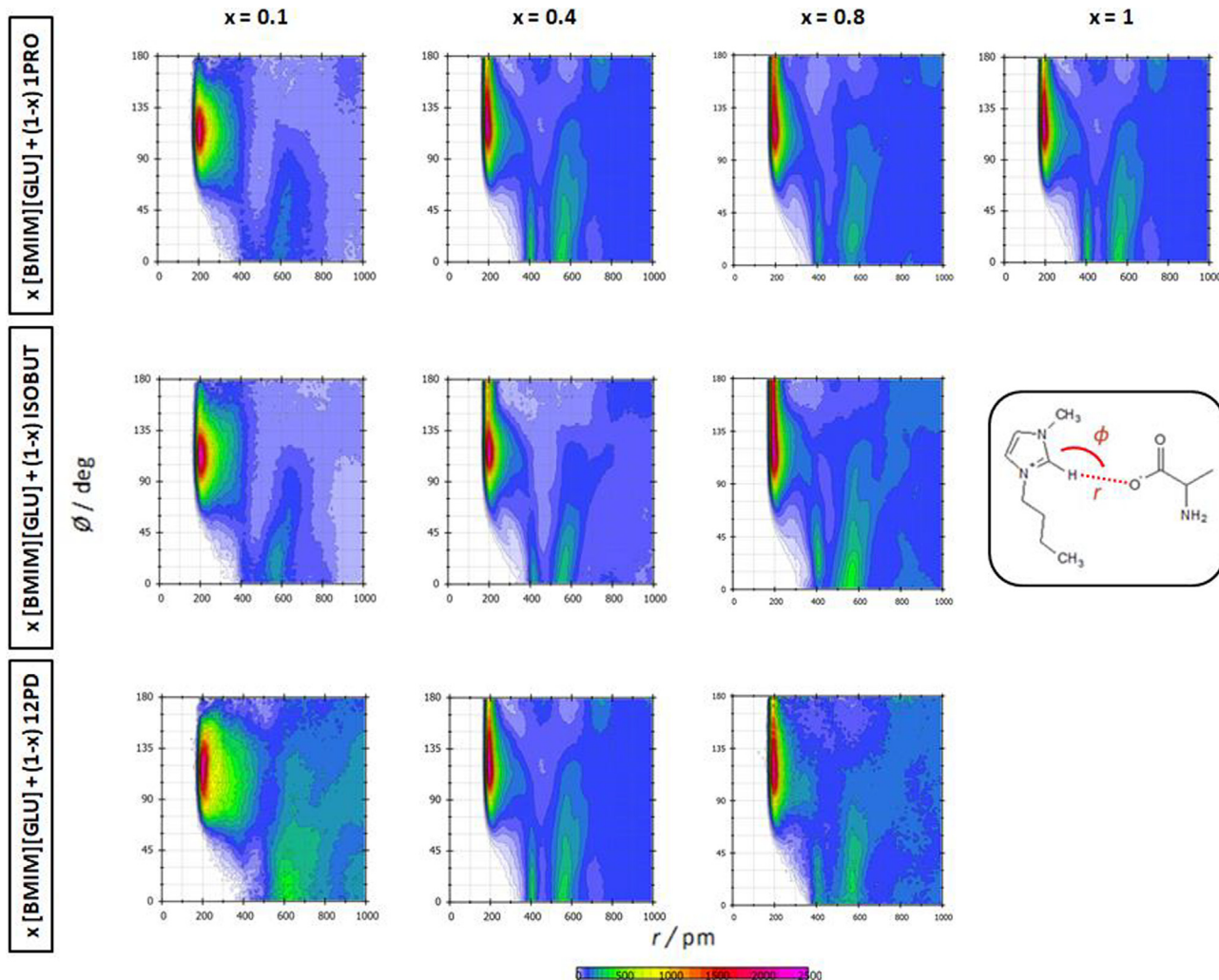


Fig. 14. Spatial distribution functions of the corresponding centers-of-mass around a central [BMIM][GLU] ion for the reported mixtures at 313 K and 0.1 MPa.

ChelpG charges, Table 2, show charge transfer upon anion – cation interaction, with average charge being +/- 0.9 for [bmim] and [glu], respectively. The QTAIM analysis of anion – cation interactions show the formation of a large number of bond, (3-,1) type (BCP) according to QTAIM naming, and ring, (3,+1) type (RCP), critical points, Figure S2 (Supplementary Information). These topological critical points appear in the bond paths connecting not only the oxygen atoms of the [glu] and the CH(1) or CH(2) site in the imidazolium ring of the cation but also appear in bond paths connecting methyl and butyl sites of the cation and different sites in the [glu] anion, Figure S2 (Supplementary Information) thus contributing to the strengthening of the anion – cation interaction. The BCPs connecting the oxygen atoms in carboxylate group of [glu] and the CH(2) (BCP #75, Figure S2a, Supplementary Information) or CH(1) (BCPs #71 and #82, Figure S2a, Supplementary Information) leads to the larger values of the electron density,  $\rho_e$ , and the corresponding Laplacian,  $\nabla^2\rho_e$ , in comparison with those involves other sites, therefore indicating stronger interactions through the imidazolium sites. According to the Popelier criteria [104], an intermolecular interaction may be classified as hydrogen bond when the  $\rho_e$  and  $\nabla^2\rho_e$  for the corresponding BCPs are in the 0.002 to 0.04 a.u. and 0.020 to 0.139 a.u. ranges, respectively, with larger values indicating stronger hydrogen bonds. The  $\rho_e$  and  $\nabla^2\rho_e$  values reported in Table 3 for [bmim] – [glu] interactions through the #75, #71 and

#82 BCPs are close to the upper limits of hydrogen bonding criteria, thus confirming the development of this type of strong anion – cation intermolecular interaction. Likewise, the formation of RCPs and weaker BCPs as reported in Table 3 shows anion – cation interaction through non-hydrogen bonding sites, mainly through van der Waals interactions contributing to the total interaction energy. The RDG analysis as reported in Figure S3 (Supplementary Information) and Fig. 9 show the development of a strong interaction region in the vicinity of the CH(2) site of imidazolium ring, Fig. 9a (blue spot), corresponding to the anion – cation hydrogen bonding between the CH(2) site and the oxygen atom of the [glu] carboxylate group.

Regarding the alkanol interaction with [bmim] – [glu], clusters considering anion – cation interaction through the CH(2) imidazolium site are considered and the possible interaction sites for alkanol are studied (Figure S1b, Supplementary Information). The corresponding  $\Delta E$  values are reported in Table 2, showing strong interaction for all the considered alkanols with the anion – cation ion pair. The alkanol interaction is also characterized by a very minor charge transfer to or from the alkanol as the charges in the ions upon interaction with the alkanol are almost the same as in absence of the alkanol, Table 2. The QTAIM analysis of interactions, Figure S2 (Supplementary Information) and Table 3, shows that BCPs corresponding to [bmim] – [glu] interactions suffer



**Fig. 15.** Combined distribution functions of radial distribution functions ( $x$ -axis) and angular distribution functions ( $y$ -axis) for the reported distances,  $r$ , and angles,  $\phi$ , (cation-anion interactions) for  $x$  [BMIM][GLU] +  $(1-x)$  1PRO/ISOBUT/12PD mixtures at 313 K and 0.1 MPa.

almost negligible changes, in terms of  $\rho_e$  and  $\nabla^2\rho_e$ , upon interaction with alkanol molecules. Therefore, the anion – cation hydrogen bonding through the CH(2) sites is maintained, not weakened, in presence of the alkanol molecules. Likewise, the BCPs corresponding to the alkanol – ions interactions show lower  $\rho_e$  and  $\nabla^2\rho_e$  values in comparison with those for anion – cation ones, and although being in the hydrogen bonding range show weaker interactions. Therefore, alkanol – ion interactions are true hydrogen bonds but allow the simultaneous anion – cation strong interaction through hydrogen bonding. The RDG analysis of alkanol – ion pair interactions are reported in Fig. 9 and Figure S3 (Supplementary Information) for interactions through site #4 (Figure S2, Supplementary Information). The reported RDG results confirm the [bmim] – [glu] hydrogen bonding (blue spots in the vicinity of CH(2) imidazolium site) with minor changes, slight weakening, when compared with the ion pair in absence of alkanol. Likewise, RDG blue spots in regions between [glu] anion and alkanol molecules confirm the development of hydrogen bonding for the alkanol. Likewise, the formation of large regions corresponding to van der Waals – like interactions (green spots) show that this type of interactions contributes to the large  $\Delta E$  values reported in Table 2 in parallel with hydrogen bonding in spite of the moderate  $\rho_e$  and  $\nabla^2\rho_e$  values reported in Table 3 for ion – alkanol BCPs. Moreover, the large RDG can der Waals regions are in parallel to

the formation of RCPs according to the QTAIM approach, which contribute to the strengthening of ion – alkanol interactions without weakening anion – cation intermolecular forces.

### 3.4. Molecular modelling: MD

The structuring of the studied [bmim] – [glu] + alkanol mixtures was analyzed using classical MD simulations. The considered MD forcefield allowed a suitable description of relevant physicochemical properties such as density. The comparison between experimental and MD predicted density (Figure S4, Supplementary Information), shows how the model allows to predict the effect of the type of alkanol as well as the complex non-linear composition effect on the property.

The nanoscopic structuring of the studied complex liquids mixtures should have its roots on the possible hydrogen bonding between the available hydrogen bonding donor and acceptor sites. For this purpose, Radial Distribution Functions (RDFs) were calculated for all the possible donor – acceptor sites, considering both homo (IL – IL and alkanol – alkanol) and heteroassociations (IL – alkanol). The first peak of each RDF was considered, as being the one characterizing the possible hydrogen bonds, and these peaks were characterized by the interatomic (donor – acceptor) distance as well as for the peak intensity. All the peaks were systematically

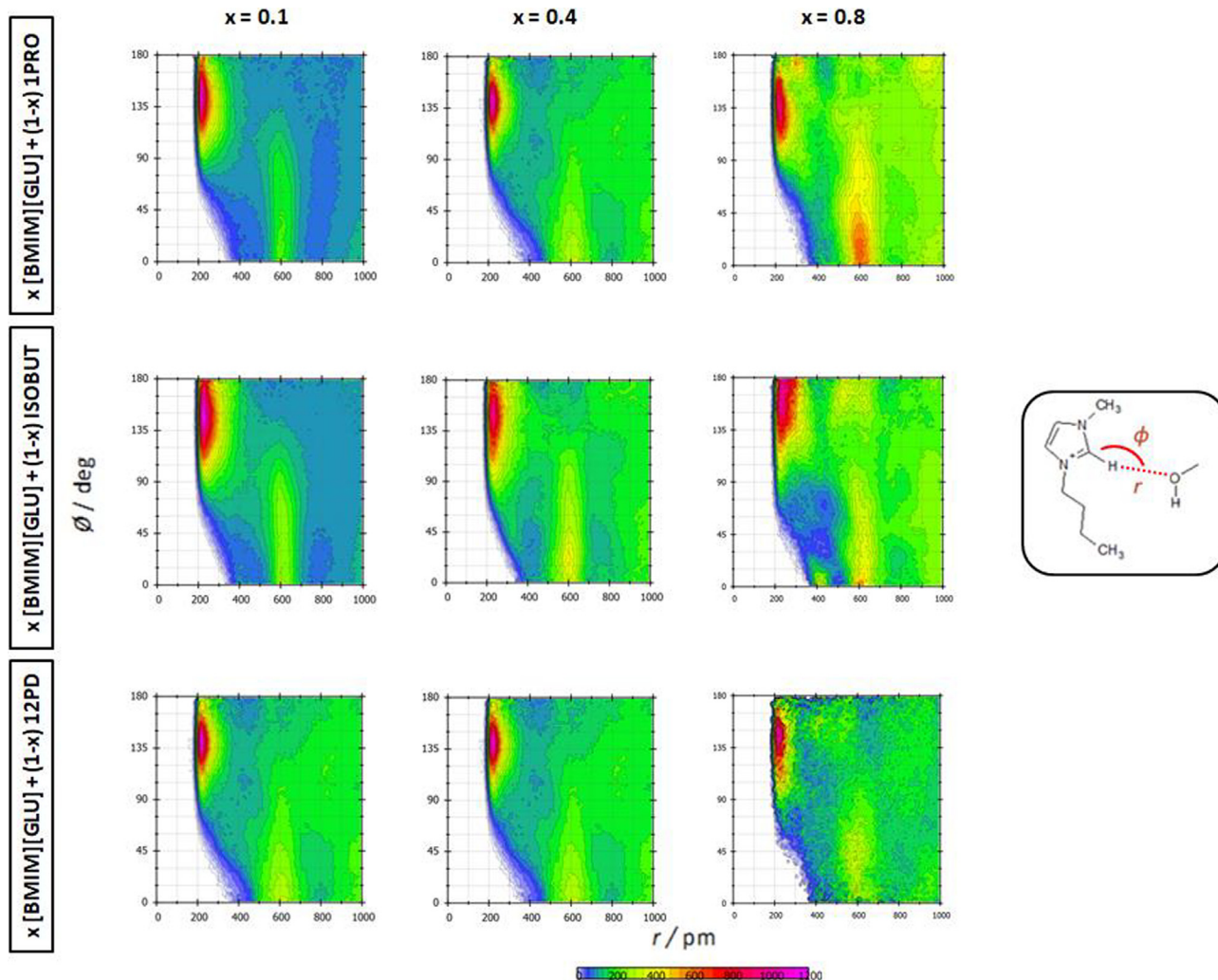


**Fig. 16.** Combined distribution functions of radial distribution functions ( $x$ -axis) and angular distribution functions ( $y$ -axis) for the reported distances,  $r$ , and angles,  $\phi$ , (cation-alkanol interactions) for  $x$  [BMIM][GLU] +  $(1-x)$  1PRO/ISOBUT/12PD mixtures at 313 K and 0.1 MPa.

arranged in a matrix, named connection matrix, in which interactions are assigned a color code according to the RDF peak height and distance. In this way all the possible interactions can be visualized and classified allowing to infer the most intense ones, being those corresponding to possible hydrogen bonds. Connection matrix results reported in Fig. 10 allow to infer: i) [bmim] – [bmim] self-interactions are negligible for all the considered systems, ii) [glu] – [glu] associations are developed, iii) regarding [bmim] – [glu] pairs, the interactions are developed through the CH(2) site in the cation, with all the possible [glu] acceptor sites (very minor differences among the available O sites in the anion), iv) [glu] – alkanol are also hydrogen bonded through all the [glu] sites (oxygen and nitrogen), and v) [bmim] – alkanol are also hydrogen bonded through the cation CH(2) site. In the case of 12PD mixtures, there are not remarkable differences between primary and secondary hydroxyl groups, both interacting with the cation as well as with anion. Therefore, alkanol molecules are able to be hydrogen bonded both with [bmim] and [glu], thus competing with the [bmim] – [glu] interactions through the cation CH(2) site.

The particular properties of relevant RDFs (those leading to possible hydrogen bonds as inferred from the connection matrix analysis) are reported in Figure 11 for the three studied alkanols and

the whole composition range. In the case of [bmim] – [glu] interactions through cation CH(2) site, Figures 11a to 11c, a first peak at 2.05 Å indicates hydrogen bonding. This peak is followed by a wide shoulder and a second peak at roughly 6 Å. The main difference between the considered alkanols stands on the intensity of the first peak as well as in the shape of the second peak. The integration of the RDFs leads to the solvation numbers,  $N$ , reported in Figure 12a for cation – anion interactions. A non-linear evolution with composition is inferred for the three studied alkanols, which is on the roots of the non-ideal behavior inferred from experimental measurements reported in previous sections. Likewise, whereas the behavior of 1PRO and ISOBUT containing mixtures is almost equivalent, mixtures with 12PD show remarkably lower  $N$  values for cation – anion interactions, especially for low IL content. Therefore, the presence of two hydroxyl groups in 12PD leads to a larger disruption of [bmim] – [glu] association in comparison with 1PRO and ISOBUT. Regarding the cation – alkanol interactions, Figures 11d–11g, a wide peak at 2.2 Å indicates hydrogen bonding, likewise a second peak at roughly 6 Å indicates the presence of neighbor alkanol molecules hydrogen bonded to the anion. The  $N$  values for cation – alkanol reported in Fig. 12b confirm the hydrogen bonding although vanishing with increasing IL content, leading to isolated alkanol monomers for IL – rich solutions. The number of cation –

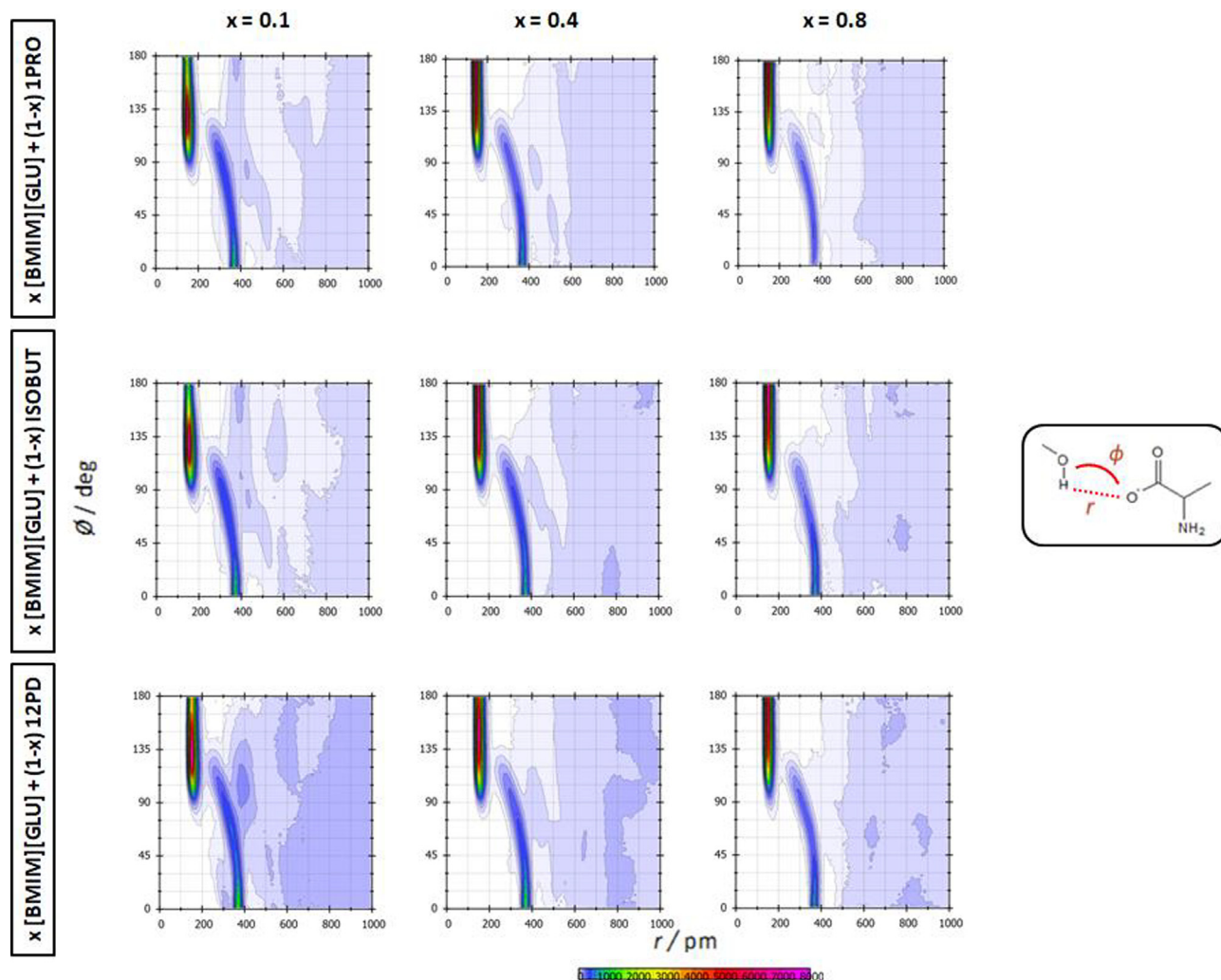


**Fig. 17.** Combined distribution functions of radial distribution functions ( $x$ -axis) and angular distribution functions ( $y$ -axis) for the reported distances,  $r$ , and angles,  $\phi$ , (anion-alkanol interactions) for  $x$  [BMIM][GLU] +  $(1-x)$  1PRO/ISOBUT/12PD mixtures at 313 K and 0.1 MPa.

alkanol interactions is lower for 12PD mixtures than for the monohydroxylic alkanols. In the case of anion – alkanol interaction, a very sharp and narrow first peak at roughly 1.6 Å confirms the hydrogen bonding, the second peak would correspond to alkanols interacting with the cation. The  $N$  numbers, Fig. 12c, confirms the development of [glu] – alkanol interactions. The comparison of results in Fig. 12b and 12c show a very different behavior depending on the IL content, for low IL content alkanol molecules are preferentially interacting with the cation whereas as the IL content increases the alkanol molecules interact with the anion. Therefore, for high IL content as the CH(2) site in the cation is hindered for the interaction with the alkanols, because of the increase of cation – anion interactions (Fig. 12a), isolated alkanol molecules interact with tails [glu] anions being involved in cation – anion clusters. The presence of two hydroxyl groups in 12PD leads to a larger number of anion – alkanol interactions, Fig. 12c. These IL – alkanol interactions are maintained beyond the first solvation shell around the interaction sites, as reported for the  $N$  numbers corresponding to the second shells in Fig. 13.

The liquid structuring is further analyzed considering Spatial Distribution Functions (SDFs) around a central [bmim] cation as a function of mixtures composition, Fig. 14. The reported SDFs are equivalent for all the considered alkanols, the alkanol and the [glu] placed around the main cation hydrogen bonding sites,

thus competing for the interaction. The distribution around the CH(2) is largely enriching with increasing IL content, as confirmed from results in Figs. 11 and 12, whereas around the cation CH(1) site alkanol molecules remains even for high IL content. Therefore, the CH(2) site leads to large interactions with the anion, whereas this site is only occupied by alkanol molecules for IL poor mixtures.

The nature of the possible hydrogen bonding is analyzed through the corresponding Combined Distribution Functions (CDFs), in which the donor – acceptor distance and orientation (angle) are simultaneously reported, Figs. 15–17. CDFs for cation – anion interactions through CH(2) site, Fig. 15. The reported red spots (indicating strong interactions) at distance – angle correspond to hydrogen bonds. These spots appear for all the considered concentration range, only a narrowing with increasing IL content is inferred, which correspond to reinforcement of cation – anion interactions for low alkanol content. In the case of cation – alkanol CDFs, Fig. 16, hydrogen bonding through CH(2) site is confirmed although weakening with increasing IL content. For the case of anion – alkanol interactions, Fig. 17, hydrogen bonding is maintained in the whole concentration range, with narrower peaks for larger IL content, thus confirming the prevailing interaction of the alkanol with the anion upon IL enrichment.

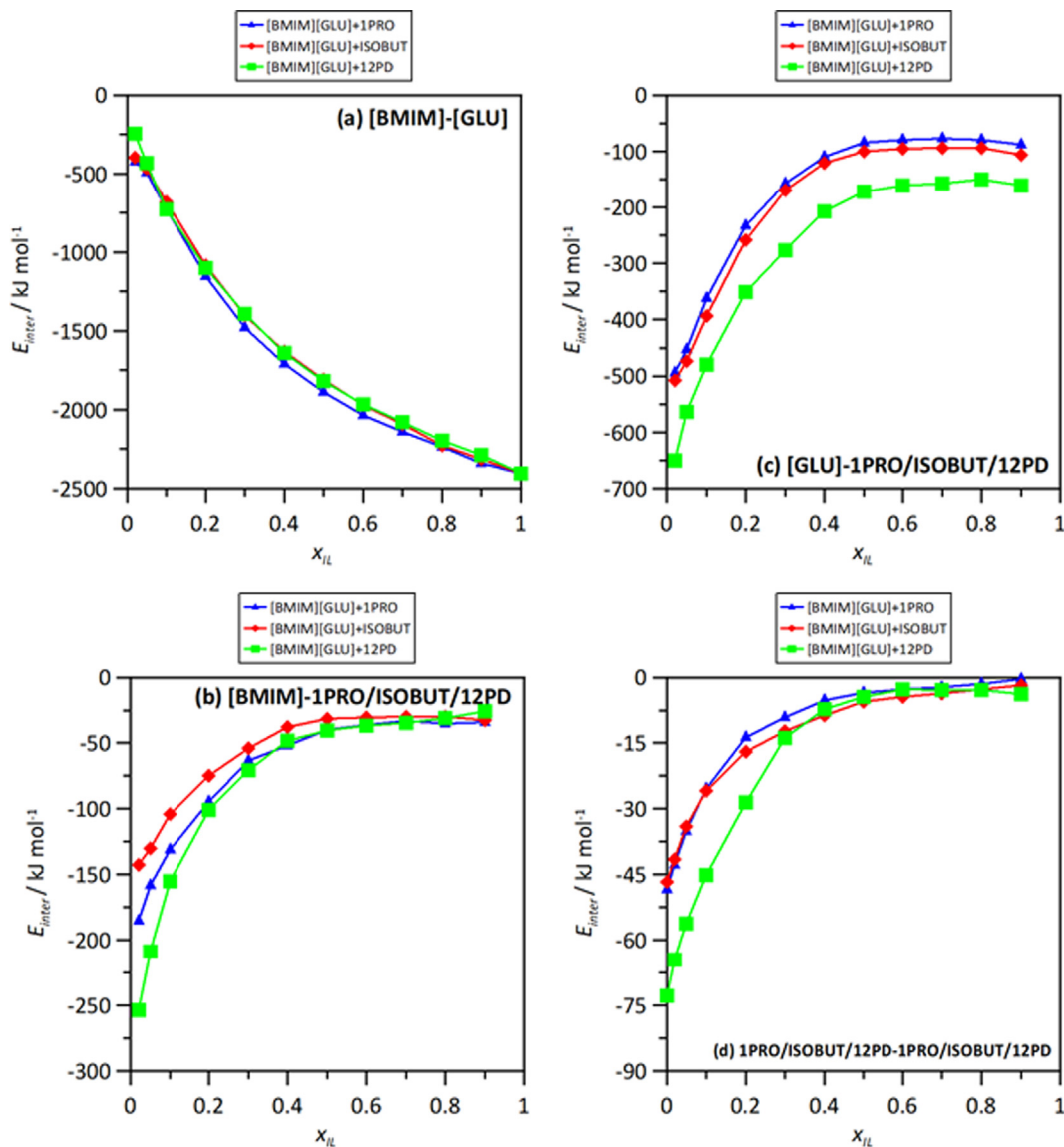


**Fig. 18.** Intermolecular interaction energy,  $E_{inter}$  (sum of Lennard-Jones and coulombic contributions), for the reported interacting pairs in  $x$  [BMIM][GLU] +  $(1-x)$  1PRO/ISOBUT/12PD mixtures at 313 K and 0.1 MPa. Symbols indicate simulation results, lines are included for guiding purposes.

The confirmed ion – alkanol interactions through hydrogen bonding may be quantified through interaction energies,  $E_{inter}$ , as a function of mixtures composition. All the possible interacting pairs show non-linear  $E_{inter}$  behavior when analyzed as a function of mixture composition, Fig. 18. The  $E_{inter}$  for cation – anion pairs are almost independent on the type of alkanol, larger values obtained with increasing IL content in agreement with the increase of ion aggregation reported in the previous sections, Fig. 18a. The behavior of  $E_{inter}$  for anion – alkanol (Fig. 18b) and cation – alkanol (Fig. 18c) is parallel, decreasing upon increasing IL content reaching an almost constant values for solutions beyond the equimolar composition. Nevertheless,  $E_{inter}$  for anion – alkanol in IL rich mixtures are larger than for cation – alkanol ones, thus showing the prevailing interactions of the alkanol with the anion for IL – rich solutions. Results in Fig. 18d show  $E_{inter}$  for alkanol – alkanol interactions, which confirm that alkanol molecules show almost negligible self-association for IL rich mixtures, thus alkanol monomers embedded into IL dominated fluids with alkanol molecules interacting preferentially with the anion is inferred.

The dynamic properties of the studied mixtures are analyzed through the self-diffusion coefficients,  $D$ , calculated from the corresponding mean square displacements ( $msd$ ) and the Einstein's equation. Calculated values of  $msd$  are reported in Figure S5 (Supplementary Information), showing proper fully diffusive behavior, which was also assured through log–log plots of  $msd$  vs. time leading to slopes in the 0.98 to 1 range. In parallel with the other experimental and theoretical properties studied in this work, the  $D$  vs. mixture composition behavior is largely non-linear. The  $D$  values are almost the same for the cation and the anion, thus showing ionic pair diffusion and it may be justified through the strong cation – anion association. Likewise, alkanol  $D$  values are close to those for the ions, which is a proof of the strong alkanol – ion heteroassociation through hydrogen bonding. The ordering for the diffusion rates for all the studied compositions is 12PD < ISOBUT < 1PRO, Fig. 19, which agrees with the  $E_{inter}$  behavior reported in Fig. 18. Therefore, the molecular mobility is largely conditioned by the trend to develop anion – cation association, with only remarkable alkanol disrupting effect for large alkanol content.

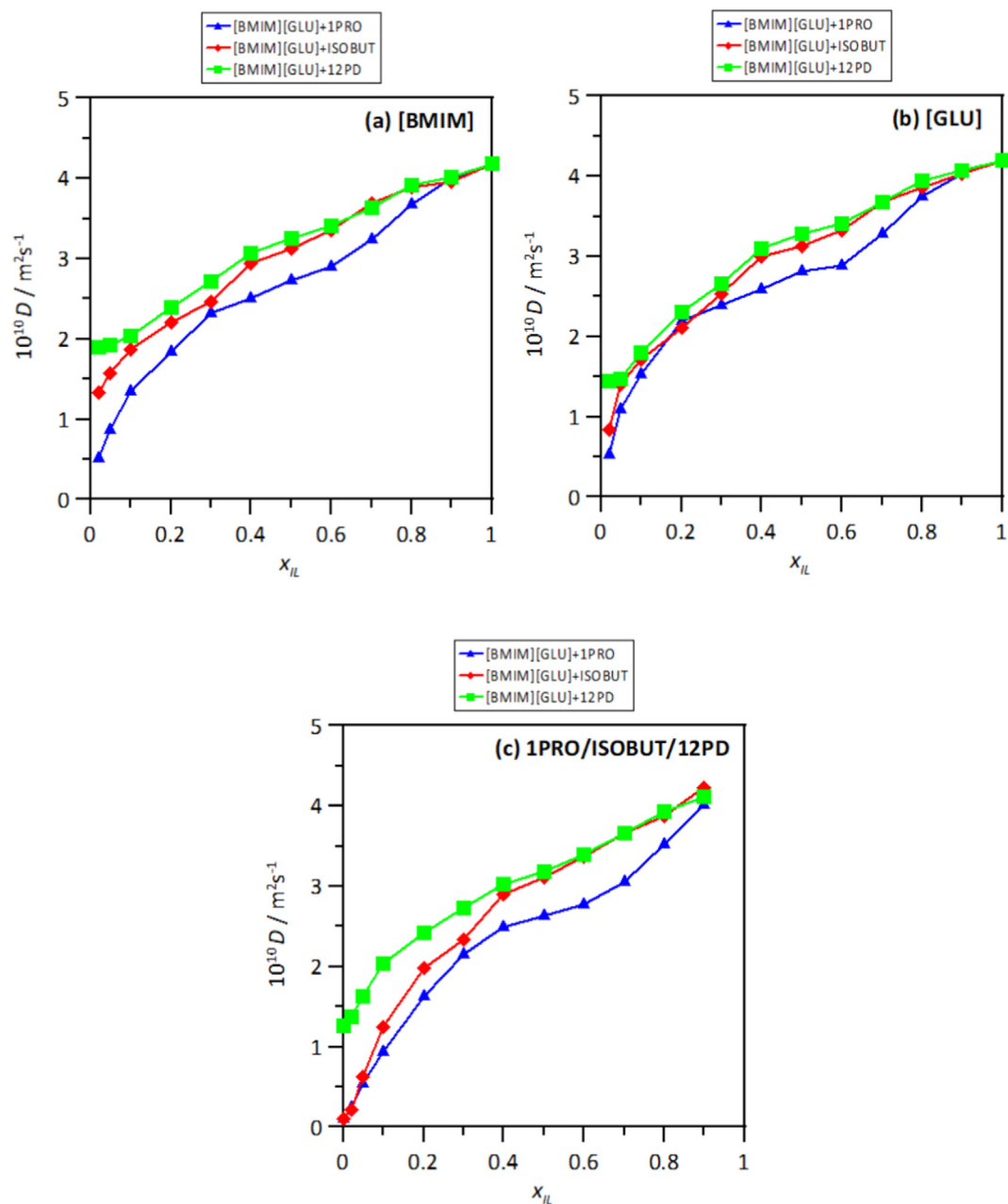


**Fig. 19.** Self-diffusion coefficient (calculated from msd using Einstein's equation),  $D$ , for (a) cation, (b) anion and (c) alkanol in  $x$  [BMIM][GLU] +  $(1-x)$  1PRO/ISOBUT/12PD mixtures at 313 K and 0.1 MPa. Values are calculated for corresponding centers-of-mass. Symbols indicate simulation results, lines are included for guiding purposes.

#### 4. Conclusions

The micro and macroscopic properties of [bmim][glu] + alkanol mixtures have been studied using a combined experimental and theoretical approach. The studied mixtures are predicted to be safe from ecotoxicological viewpoint with alkanol making safer fluids in comparison with the neat ionic liquid. The reported experimental results show two main factors controlling the structuring of these systems: *i*) the difference in the volumetric properties, i.e. steric effects, between the ionic liquid and the alkanols, larger for simple, monohydroxylic alkanols, and *ii*) the number of hydroxyl groups in the alkanol controlling self- and hetero-aggregation through hydrogen bonding. These two factors lead contractive mixing and large ionic liquid to alkanol hydrogen bonding. The molecular bonding studies confirmed the availability of alkanol molecules to be hydrogen bonded with ions sites. Nevertheless,

the large trend to develop anion – cation pairs has a large disruptive effect on alkanols self-association. Therefore, ionic liquid – rich mixtures are characterized by the interaction of alkanol monomers with large ionic clusters, especially with anion, whereas for low ionic liquid content alkanols remains self-associated but also interacting with the available ions. Hence, the transition from prevailing alkanols self-associated fluids to fluids with self-associated ionic liquid determines the physicochemical properties of the studied mixed solvents.

#### Declaration of Competing Interest

The authors declare that they have no known competing financial interests or personal relationships that could have appeared to influence the work reported in this paper.

## Acknowledgements

This work was funded by Shiraz University of Technology and Ministerio de Ciencia, Innovación y Universidades (Spain, project RTI2018-101987-B-I00). We also acknowledge SCAYLE (Supercomputación Castilla y León, Spain) for providing supercomputing facilities. The statements made herein are solely the responsibility of the authors.

## Appendix A. Supplementary data

Supplementary data to this article can be found online at <https://doi.org/10.1016/j.molliq.2021.117953>.

## References

- [1] S.K. Singh, A.W. Savoy, Ionic liquids synthesis and applications: An overview, *J. Mol. Liq.* 297 (2020) 112038, <https://doi.org/10.1016/j.molliq.2019.112038>.
- [2] N. Narsipour, M. Mohammadporfard, S.Z. Heris, Ionic liquids: Promising compounds for sustainable chemical processes and applications, *Chem. Eng. Res. Des.* 160 (2020) 264–300.
- [3] G. Cevasco, C. Chiappe, Are ionic liquids a proper solution to current environmental challenges?, *Green Chem* 16 (2014) 2375–2385.
- [4] R.S. Kalb, Toward Industrialization of Ionic Liquids. In: Shiflett M. (eds) *Commercial Applications of Ionic Liquids*. Green Chemistry and Sustainable Technology. 2020, Springer, Cham. [https://doi.org/10.1007/978-3-030-35245-5\\_11](https://doi.org/10.1007/978-3-030-35245-5_11)
- [5] M. Bystrzanowska, F. Pena-Pereira, Ł. Marcinkowski, M. Tobiszewski, How green are ionic liquids? – A multicriteria decision analysis approach, *Ecotox. Environ. Safe.* 174 (2019) 455–458.
- [6] S. Magina, A. Barros-Timmons, P.M. Ventura, D.V. Evtuguin, Evaluating the hazardous impact of ionic liquids – Challenges and opportunities, *J. Hazard. Mater.* 412 (2021) 125215.
- [7] S.P.F. Costa, A.M.O. Azevedo, P.C.A.G. Pinto, L.M.F.S. Saraiva, Environmental Impact of Ionic Liquids: Recent Advances in (Eco)toxicology and (Bio) degradability, *ChemSusChem* 10 (2017) 2321–2347.
- [8] P.G. Jessop, Fundamental properties and practical applications of ionic liquids: concluding remarks, *Faraday Discuss.* 206 (2018) 587–601.
- [9] P.G. Jessop, Searching for green solvents, *Green Chem.* 13 (6) (2011) 1391, <https://doi.org/10.1039/c0gc00797h>.
- [10] F.M. Perna, P. Vitale, V. Capriati, Deep eutectic solvents and their applications as green solvents, *Curr. Opin. Green Sus. Chem.* 21 (2020) 27–33.
- [11] A.P.R. Santan, J.A. Mora-Vargas, T.G.S. Guimaraes, C.D.B. Amaral, A. Oliveira, M.H. Gonzalez, Sustainable synthesis of natural deep eutectic solvents (NADES) by different methods, *J. Mol. Liq.* 293 (2019) 111452.
- [12] Z. Song, X. Hu, H. Wu, M. Mei, S. linke, T. Zhou, Z. Qi, K. Sundmacher, *ACS Sus. Chem.* 8 (2020) 8741–8751.
- [13] Benworth B. Hansen, Stephanie Spittle, Brian Chen, Derrick Poe, Yong Zhang, Jeffrey M. Klein, Alexandre Horton, Laxmi Adhikari, Tamar Zelovich, Brian W. Doherty, Burcu Gurkan, Edward J. Maginn, Arthur Ragauskas, Mark Dardun, Thomas A. Zawodzinski, Gary A. Baker, Mark E. Tuckerman, Robert F. Savinell, Joshua R. Sangoro, Deep Eutectic Solvents: A Review of Fundamentals and Applications, *Chem. Rev.* 121 (3) (2021) 1232–1285.
- [14] G. Chatel, E. Naffrechoux, M. Draye, Avoid the PCB mistakes: A more sustainable future for ionic liquids, *J. Hazard. Mater.* 324 (2017) 773–780.
- [15] J. Feder-Kubis, P. Czerwoniec, P. Lewandowski, H. Pospieszny, M. Smiglak, Ionic liquids with natural origin component: a path to new plant protection products, *ACS Sustainable Chem.* 8 (2020) 842–852.
- [16] J.M. Gomes, S.S. Silva, R.L. Reis, Biocompatible ionic liquids: fundamental behaviours and applications, *Chem. Soc. Rev.* 48 (2019) 4317–4335.
- [17] L. Gontrani, Choline-amino acid ionic liquids: past and recent achievements about the structure and properties of these really “green” chemicals, *Biophys. Rev.* 10 (2018) 873–880.
- [18] Shubhankar Bhattacharyya, Faiz Ullah Shah, Thermal stability of choline based amino acid ionic liquids, *J. Mol. Liq.* 266 (2018) 597–602.
- [19] Ying-Ying Jiang, Guan-Nan Wang, Zheng Zhou, You-Ting Wu, Jiao Geng, Zhi-Bing Zhang, Tetraalkylammonium amino acids as functionalized ionic liquids of low viscosity, *Chem. Comm.* (4) (2008) 505–507, <https://doi.org/10.1039/B713648J>.
- [20] Ling He, Guo-Hong Tao, Damon A. Parrish, Jean’ne M. Shreeve, Slightly viscous amino acid ionic liquids: synthesis, properties, and calculations, *J. Phys. Chem. B* 113 (46) (2009) 15162–15169.
- [21] P. Ossowicz, J. Klebeko, B. Roman, E. Janus, Z. Rozwadowski, The relationship between the structure and properties of amino acid ionic liquids, *Molecules* 24 (2018) 3252.
- [22] Xue-Dan Hou, Qiu-Ping Liu, Thomas J. Smith, Ning Li, Min-Hua Zong, Vipul Bansal, Evaluation of Toxicity and Biodegradability of Cholinium Amino Acids Ionic Liquids, *PLOS One* 8 (3) (2013) e59145, <https://doi.org/10.1371/journal.pone.0059145>.
- [23] Shuai Zhang, Lin Ma, Ping Wen, Xiangyuan Ye, Rui Dong, Wenjing Sun, Mingjin Fan, Desuo Yang, Feng Zhou, Weimin Liu, The ecotoxicity and tribological properties of choline amino acid ionic liquid lubricants, *Tribol. Int.* 121 (2018) 435–441.
- [24] Shuanggen Wu, Fenfang Li, Liangbin Zeng, Chaoyun Wang, Yuanru Yang, Zhijian Tan, Assessment of the toxicity and biodegradation of amino acid-based ionic liquids, *RSC Adv.* 9 (18) (2019) 10100–10108.
- [25] A.R. Shaikh, M. Ashraf, T. AlMayef, M. Chawla, A. Poater, L. Cavallo, Amino acid ionic liquids as potential candidates for CO<sub>2</sub> capture: Combined density functional theory and molecular dynamics simulations, *Chem. Phys. Lett.* 745 (2020) 137239.
- [26] Ponnkantani Nagendramma, Praveen K. Khatri, Ganath D. Thakre, Suman L. Jain, Lubrication capabilities of amino acid based ionic liquids as green bio-lubricant additives, *J. Mol. Liq.* 244 (2017) 219–225.
- [27] D.K. Shao, S. Jena, K.D. Tulsian, J. Dutta, S. Chakrabarty, H.S. Biswal, Amino-acid-based ionic liquids for the improvement in stability and activity of cytochrome c: a combined experimental and molecular dynamics study, *J. Phys. Chem. B* 123 (2019) 10100–10109.
- [28] M.R. Islam, M.R. Chowdhury, R. Wakabayashi, Y. Tahara, N. Kamiya, M. moniruzzaman, M. Goto, *Int. J. Pharm.* 582 (2020) 1129335.
- [29] Heiko Niedermeyer, Jason P. Hallett, Ignacio J. Villar-Garcia, Patricia A. Hunt, Tom Welton, Mixtures of ionic liquids, *Chem. Soc. Rev.* 41 (23) (2012) 7780, <https://doi.org/10.1039/c2cs35177c>.
- [30] P. Dhakal, J.K. Shah, Recent advances in molecular simulations of ionic liquid-ionic liquid mixtures, *Curr. Opin. Green. Sus. Chem.* 18 (2019) 90–97.
- [31] V.V. Chaban, O.V. Prezhdo, Ionic and molecular liquids: working together for robotics engineering, *J. Phys. Chem. Lett.* 4 (2013) 1423–1431.
- [32] Karina Pivnic, Fernando Bresme, Alexei A. Kornyshev, Michael Urbakh, Structural forces in mixtures of ionic liquids with organic solvents, *Langmuir* 35 (47) (2019) 15410–15420.
- [33] Jinlei Cui, Takeshi Kobayashi, Robert L. Sacci, Ray A. Matsumoto, Peter T. Cummings, Marek Pruski, Diffusivity and structure of room temperature ionic liquid in various organic solvents, *J. Phys. Chem. B* 124 (44) (2020) 9931–9937.
- [34] Y. Kohno, H. Ohno, Ionic liquid/water mixtures: from hostility to conciliation, *Chem. Comm.* 48 (2012) 7119–7130.
- [35] José M. Otero-Mato, Volker Lesch, Hadrián Montes-Campos, Jens Smiatek, Diddo Diddens, Oscar Cabeza, Luis J. Gallego, Luis M. Varela, Solvation in ionic liquid-water mixtures: A computational study, *J. Mol. Liq.* 292 (2019) 111273, <https://doi.org/10.1016/j.molliq.2019.111273>.
- [36] A. Verma, J.P. Stippelman, J.G. McDaniel, Tuning Water Networks via Ionic Liquid/Water Mixtures, *Int. J. Mol. Sci.* 21 (2020) 403.
- [37] A.M. Smith, A.A. Lee, S. Perkin, Switching the structural force in ionic liquid-solvent mixtures by varying composition, *Phys. Rev. Lett.* 118 (2017) 096002.
- [38] H.J. Jiang, R. Atkin, F.G. Varr, Nanostructured ionic liquids and their solutions: Recent advances and emerging challenges, *Curr. Opin. Green Sus. Chem.* 12 (2018) 27–32.
- [39] Matthew W. Thompson, Ray Matsumoto, Robert L. Sacci, Nicolette C. Sanders, Peter T. Cummings, Scalable screening of soft matter: a case study of mixtures of ionic liquids and organic solvents, *J. Phys. Chem. B* 123 (6) (2019) 1340–1347.
- [40] P.M. Mancini, G.G. Fortunato, L.R. Vottero, Molecular solvent/ionic liquid binary mixtures: designing solvents based on the determination of their microscopic properties, *Phys. Chem. Liq.* 42 (2004) 625–632.
- [41] S.N. Mirheydari, J. Soleymani, V.J. Gharamaleki, M.B. Jalali, A. Jouyban, H. Shekaari, Viscosity prediction of ionic liquid + molecular solvent mixtures at various temperatures, *J. Mol. Liq.* 263 (2018) 228–236.
- [42] J.C. Araque, J.J. Hettige, C.J. Margulis, Ionic Liquids-Conventional Solvent Mixtures, Structurally Different but Dynamically Similar, *J. Chem. Phys.* 143 (2015) 134505.
- [43] D.R. MacFarlane, A.L. Chong, M. Forsyth, M. Kar, R. Vijayaraghavan, A. Somers, J.M. Pringle, New dimensions in salt-solvent mixtures: a 4th evolution of ionic liquids, *Faraday Discuss.* 206 (2018) 9–28.
- [44] M. Tariq, K. Shimizu, J.M.S.S. Esperanca, J.N. Canongia-Lopes, L.P.N. Rebelo, Viscosity minima in binary mixtures of ionic liquids + molecular solvents, *Phys. Chem. Chem. Phys.* 17 (2015) 13480–13494.
- [45] Fuxin Yang, Xiaopo Wang, Houzhang Tan, Zhigang Liu, Improvement the viscosity of imidazolium-based ionic liquid using organic solvents for biofuels, *J. Mol. Liq.* 248 (2017) 626–633.
- [46] G. Raabe, J. Kohler, Thermodynamical and structural properties of binary mixtures of imidazolium chloride ionic liquids and alcohols from molecular simulation, *J. Chem. Phys.* 129 (2008) 144503.
- [47] Ray Matsumoto, Matthew W. Thompson, Peter T. Cummings, Ion pairing controls physical properties of ionic liquid-solvent mixtures, *J. Phys. Chem. B* 123 (46) (2019) 9944–9955.
- [48] Dilek Yalcin, Andrew J. Christofferson, Calum J. Drummond, Tamar L. Greaves, Solvation properties of protic ionic liquid-molecular solvent mixtures, *Phys. Chem. Chem. Phys.* 22 (19) (2020) 10995–11011.
- [49] J.M. Otero-Mato, V. Lesch, H. Montes – Campos, J. Smiatek, D. Diddens, O. Cabeza, L.M. Varela, Solvation in ionic liquid-water mixtures: A computational study, *J. Mol. Liq.* 2019, 292, 111273.
- [50] Z. Khedri, M. Almasi, A. Maleki, Kirkwood-Buff integrals and structure factor for binary mixtures of ionic liquid with 1-alkanol, *J. Mol. Liq.* 296 (2019) 111767.
- [51] Q. Zhang, D. Liu, Q. Li, X. Zhang, Y. Wei, X. Lang, Thermodynamic properties, excess properties, and molecular interactions of ionic liquids 1-cyanopropyl-3-methyl-imidazolium bisfluorosulfonylimide/trifluoromethanesulfonate and binary systems containing acetonitrile, *J. Mol. Liq.* 268 (2018) 770–780.
- [52] O. Cocirlan, O. Croitoru, O. Iulian, Viscosity of binary mixtures of 1-ethyl-3-methylimidazolium tetrafluoroborate ionic liquid with four organic solvents, *J. Chem. Thermodyn.* 101 (2016) 285–292.

- [53] Umme Salma, Paolo Ballirano, Marianna Usula, Ruggero Caminiti, Natalia V. Plechkova, Kenneth R. Seddon, Lorenzo Contrani, A new insight into the nanostructure of alkylammonium alkanolates based ionic liquids in water, *Phys. Chem. Chem. Phys.* 18 (16) (2016) 11497–11502.
- [54] Ashley J. Holding, Arno Parviainen, Ilkka Kilpeläinen, Ana Soto, Alistair W.T. King, Héctor Rodríguez, Efficiency of hydrophobic phosphonium ionic liquids and DMSO as recyclable cellulose dissolution and regeneration media, *RSC Adv.* 7 (28) (2017) 17451–17461.
- [55] C. Herrera, R. Alcalde, M. Atilhan, S. Aparicio, Microscopic characterization of mixtures of amino acid ionic liquids and organic solvents, *J. Mol. Liq.* 250 (2019) 111–120.
- [56] P. Pavez, R. Figueroa, M. Medina, D. Millan, D. Falcione, R.A. Tapia, Choline [Amino Acid] Ionic Liquid/Water Mixtures: A Triple Effect for the Degradation of an Organophosphorus Pesticide, *ACS Omega* 5 (2020) 26562–26572.
- [57] M. Taghizadehfard, S.M. Hosseini, M. Pierantozzi, M.M. Alavianmehr, Predicting the volumetric properties of pure and mixture of amino acid-based ionic liquids, *J. Mol. Liq.* 294 (2019) 111604.
- [58] R.P. Swatoski, J.D. Holbrey, R.D. Rogers, Ionic liquids are not always green: hydrolysis of 1-butyl-3-methylimidazolium hexafluorophosphate, *Green Chem.* 5 (2003) 361–363.
- [59] Z. Song, Y. Liang, M. Fan, F. Zhou, W. Liu, Ionic liquids from amino acids: fully green fluid lubricants for various surface contacts, *RSC Adv.* 4 (2014) 19396–19402.
- [60] Wei Guan, Jing Tong, San-Ping Chen, Qing-Shan Liu, Sheng-Li Gao, Density and surface tension of amino acid ionic liquid 1-alkyl-3-methylimidazolium glutamate, *J. Chem. Eng. Data* 55 (9) (2010) 4075–4079.
- [61] Ying Wei, Qing-Guo Zhang, Yang Liu, Xiaorui Li, Suoyuan Lian, Zhenhui Kang, Physicochemical Property Estimation of an Ionic Liquid Based on Glutamic Acid-BMI-Glu, *J. Chem. Eng. Data* 55 (7) (2010) 2616–2619.
- [62] Kenta Fukumoto, Masahiro Yoshizawa, Hiroyuki Ohno, Room temperature ionic liquids from 20 natural amino acids, *J. Am. Chem. Soc.* 127 (8) (2005) 2398–2399.
- [63] Ying Wei, Qing-Guo Zhang, Yang Liu, Xiaorui Li, Suoyuan Lian, Zhenhui Kang, Physicochemical property estimation of an ionic liquid based on glutamic acid–BMI-Glu, *J. Chem. Eng. Data* 55 (7) (2010) 2616–2619.
- [64] Z. Wagner, M. Bendova, J. Rotrekl, S. Orvalho, Densities, vapour pressures, and surface tensions of selected terpenes, *J. Sol. Chem.* 48 (2019) 1147–1166.
- [65] Z. Wagner, M. Bendova, J. Rotrekl, A. Sykorova, M. Canji, N. Parmar, Density and sound velocity measurement by an Anton Paar DSA 5000 density meter: Precision and long-time stability, *J. Mol. Liq.* 329 (2021) 115547.
- [66] Haiyan Gao, Zhichao Yu, Haijun Wang, Densities and volumetric properties of binary mixtures of amino acid ionic liquid [bmim][Glu] or [bmim][Gly] with benzylalcohol at T=(298.15 to 313.15) K, *J. Chem. Thermodyn.* 42 (5) (2010) 640–645.
- [67] Jacobo Troncoso, Clara A. Tovar, Claudio A. Cerdeiriña, Enrique Carballo, Luís Romani, Temperature dependence of densities and speeds of sound of nitromethane+ butanol isomers in the range (288.15–308.15) K, *J. Chem. Eng. Data* 46 (2) (2001) 312–316.
- [68] Divna M. Majstorović, Emila M. Živković, Mirjana Lj. Kijevčanin, Density, viscosity, and refractive index data for a ternary system of wine congeners (ethyl butyrate+ diethyl succinate+ isobutanol) in the temperature range from 288.15 to 323.15 K and at atmospheric pressure, *J. Chem. Eng. Data* 62 (1) (2017) 275–291.
- [69] F. Kermanpour, H.Z. Niakan, Experimental excess molar properties of binary mixtures of (3-amino-1-propanol+ isobutanol, 2-propanol) at T=(293.15 to 333.15) K and modelling the excess molar volume by Prigogine–Flory–Patterson theory, *J. Chem. Thermodynamics* 54 (2012) 10–19.
- [70] Elisa Langa, Ana M. Mainar, Juan I. Pardo, José S. Urieta, Excess enthalpy, density, and speed of sound for the mixtures β-pinene+ 2-methyl-1-propanol or 2-methyl-2-propanol at several temperatures, *J. Chem. Eng. Data* 52 (6) (2007) 2182–2187.
- [71] Balwinder Saini, Ashwani Kumar, Ruby Rani, Rajinder K. Bamezai, Thermodynamic and acoustical properties of mixtures p-anisaldehyde–alkanols (C 1–C 4)–2-methyl-1-propanol at 303.15 K, *Russian J. Phys. Chem. A* 90 (7) (2016) 1350–1361.
- [72] F. Kermanpour, T.S. Etefagh, H. Iloukhani, Measurement and calculation the excess molar properties of binary mixtures containing isobutanol, 1-amino-2-propanol, and 1-propanol at temperatures of (293.15 to 333.15) K, *J. Sol. Chem.* 46 (2) (2017) 446–460.
- [73] Lihu Dong, Jian Chen, Guanghua Gao, Solubility of carbon dioxide in aqueous solutions of 3-amino-1-propanol, *J. Chem. Eng. Data* 55 (2) (2010) 1030–1034.
- [74] M. Ramos-Estrada, I.Y. López-Cortés, G.A. Iglesias-Silva, F. Pérez-Villaseñor, Density, Viscosity, and Speed of Sound of Pure and Binary Mixtures of Ionic Liquids Based on Sulfonium and Imidazolium Cations and Bis (trifluoromethylsulfonyl) imide Anion with 1-Propanol, *J. Chem. Eng. Data* 63 (2018) 4425–4444.
- [75] Francisca Maria Rodrigues Mesquita, Laís Lopes Coelho, Regiane Silva Pinheiro, Carlos Augusto Russo Costa Ribeiro, Filipe Xavier Feitosa, Hosierto Batista de Sant’Ana, Rílvia Saraiva de Santiago-Aguiar, Santiago-Aguiar, Liquid Densities and Speed of Sound for Ionic Liquid (2-HEAA and 2-HDEAA)+ Alcohol (1-Propanol and 2-Propanol) Mixtures at T=(293.15–323.15 K) and Atmospheric Pressure, *J. Chem. Eng. Data* 64 (8) (2019) 3316–3322.
- [76] Xiaojie Wang, Xiaopo Wang, Dongbo Wang, Volumetric and viscometric properties of ethyl caprate+ 1-propanol,+ 1-butanol, and+ 1-pentanol from 283.15 K to 318.15 K, *J. Mol. Liq.* 225 (2017) 311–319.
- [77] Fuxin Yang, Xiaopo Wang, Houzhang Tan, Siyuan He, Zhigang Liu, Experimental investigations on the thermophysical properties of methyl myristate in alcoholic solutions, *Fuel* 215 (2018) 187–195.
- [78] Amalendu Pal, Mohit Saini, Bhupinder Kumar, Volumetric, ultrasonic and spectroscopic (FT-IR) studies for the binary mixtures of imidazolium based ILs with 1, 2-propanediol, *Fluid Phase Equilib.* 411 (2016) 66–73.
- [79] H.A. Zarei, F. Jalili, Densities and derived thermodynamic properties of (2-methoxyethanol+ 1-propanol, or 2-propanol, or 1, 2-propandiol) at temperatures from T=(293.15 to 343.15) K, *The Journal of Chemical Thermodynamics* 39 (2007) 55–66.
- [80] D.M. Bajić, G.R. Ivaniš, Z.P. Visak, E.M. Živković, S.P. Šerbanović, M.L. Kijevčanin, Densities, viscosities, and refractive indices of the binary systems (PEG200+ 1, 2-propanediol,+ 1, 3-propanediol) and (PEG400+ 1, 2-propanediol,+ 1, 3-propanediol) at (288.15 to 333.15) K and atmospheric pressure: Measurements and modeling, *The Journal of Chemical Thermodynamics* 57 (2013) 510–529.
- [81] Y. Hsiao, B.H. Su, Y.J. Tseng, Current development of integrated web servers for preclinical safety and pharmacokinetics assessments in drug development, *Brief. Bioinformatics* 22 (2021) bbaa160.
- [82] H. Yang, C. Lou, L. Sun, J. Li, Y. Cai, Z. Wang, W. Li, G. Liu, Y. Tang, AdmetSAR 2.0: web-service for prediction and optimization of chemical ADMET properties, *Bioinformatics* 35 (2019) 1067–1069.
- [83] Ajoy Kumer, Md. Wahab Khan, The effect of alkyl chain and electronegative atoms in anion on biological activity of anilinium carboxylate bioactive ionic liquids and computational approaches by DFT functional and molecular docking, *Heliyon* 7 (7) (2021) e07509, <https://doi.org/10.1016/j.heliyon.2021.e07509>.
- [84] K.K. Thasneema, M.S. Thayyil, T. Rosalin, K.K. Elyas, T. Dipin, P.K. Sahu, N.S.K. Kumar, V.C. Saheer, M. Messali, T.B. Hadda, Thermal and spectroscopic investigations on three phosphonium based ionic liquids for industrial and biological applications, *J. Mol. Liq.* 307 (2020) 112960.
- [85] F. Neese, The ORCA program system, *WIREs Comput. Mol. Sci.* 2 (2012) 73–78.
- [86] Chengteh Lee, Weitao Yang, Robert G. Parr, Development of the Colle-Salvetti correlation-energy formula into a functional of the electron density, *Phys. Rev. B* 37 (2) (1988) 785–789.
- [87] A.D. Becke, Density-functional exchange-energy approximation with correct asymptotic behavior, *Phys. Rev. A* 38 (6) (1988) 3098–3100.
- [88] A.D. Becke, Density-functional thermochemistry. III. The role of exact exchange, *J. Chem. Phys.* 98 (1993) 5648–5652.
- [89] S. Grimme, J. Antony, S. Ehrlich, H.A. Krieg, A consistent and accurate ab initio parametrization of density functional dispersion correction DFT-D for the 94 elements H-Pu, *J. Chem. Phys.* 132 (2010) 154104.
- [90] S. Simon, M. Duran, J. Dannenberg, How does basis set superposition error change the potential surfaces for hydrogen-bonded dimers?, *J. Chem. Phys.* 105 (1996) 11024.
- [91] Curt M. Breneman, Kenneth B. Wiberg, Determining atom-centered monopoles from molecular electrostatic potentials. The need for high sampling density in formamide conformational analysis, *J. Comput. Chem.* 11 (3) (1990) 361–373.
- [92] R.F.W. Bader, *Atoms in Molecules: A Quantum Theory*. 1990 Oxford
- [93] E.R. Johnson, S. Keinan, P. Mori-Sanchez, J. Contreras-García, A.J. Cohen, W. Yang, Revealing non-covalent interactions, *J. Am. Chem. Soc.* 132 (2010) 6498–6506.
- [94] T. Lu, F. Chen, Multiwfn: A multifunctional wavefunction analyzer, *J. Comput. Chem.* 33 (2012) 580–592.
- [95] A. P. Lyubartsev, A. Laaksonen, MDynaMix – a scalable portable parallel MD simulation package for arbitrary molecular mixtures. *Comput. Phys. Commun.* 2000, 128, 565–589.
- [96] L. Martínez, R. rade, E. G. Birgin, J. M. Martínez, PACKMOL: a package for building initial configurations for molecular dynamics simulations, *J. Comput. Chem.* 2009, 30, 2157–2164.
- [97] V. Zoete, M.A. Cuendet, A. Grosdidier, O. Michielin, SwissParam, a fast force field generation tool for small organic molecules, *J. Comput. Chem.* 32 (2011) 2359–2368.
- [98] M. Tuckerman, B.J. Berne, G.J. Martyna, Reversible multiple time scale molecular dynamics, *J. Chem. Phys.* 97 (1992) 1990–2001.
- [99] U.L. Essmann, M.L. Perera, T. Berkowitz, H. Darden, H. Lee, L.G. Pedersen, A smooth particle mesh Ewald method, *J. Chem. Phys.* 103 (1995) 8577–8593.
- [100] John D. Holbrey, Kenneth R. Seddon, The phase behaviour of 1-alkyl-3-methylimidazolium tetrafluoroborates; ionic liquids and ionic liquid crystals, *J. Chem. Soc., Dalton Trans* (13) (1999) 2133–2140, <https://doi.org/10.1039/a902818h>.
- [101] Jianji Wang, Anlian Zhu, Yang Zhao, Kelei Zhuo, Excess molar volumes and excess logarithm viscosities for binary mixtures of the ionic liquid 1-butyl-3-methylimidazolium hexafluorophosphate with some organic compounds, *J. Sol. Chem.* 34 (5) (2005) 585–596.
- [102] Zhichao Yu, Haiyan Gao, Haijun Wang, Lianwei Chen, Densities, excess molar volumes, and refractive properties of the binary mixtures of the amino acid ionic liquid [bmim][Gly] with 1-butanol or isopropanol at T=(298.15 to 313.15) K, *J. Chem. Eng. Data* 56 (12) (2011) 4295–4300.
- [103] H. Shekaari, M.T. Zafarani-Moattar, M. Mokhtarpour, S. Faraji, Volumetric and compressibility properties for aqueous solutions of choline chloride based deep eutectic solvents and Prigogine–Flory–Patterson theory to correlate of excess molar volumes at T = (293.15 to 308.15) K, *J. Mol. Liq.* 289 (2019) 111077.
- [104] U. Koch, P.L.A. Popelier, Characterization of C–H–O hydrogen bonds on the basis of charge density, *J. Phys. Chem.* 99 (1995) 9747–9754.